Journal of Structural Geology 30 (2008) 1572–1592

Contents lists available at ScienceDirect

Journal of Structural Geology

journal homepage: www.elsevier.com/locate/jsg

Folding with thermal–mechanical feedback

Bruce Hobbs [a,b,*], Klaus Regenauer-Lieb [a,b], Alison Ord [a,b]

[a] CSIRO Exploration and Mining, P.O. Box 1130, Bentley, WA 6102, Australia
[b] The School of Earth and Geographical Sciences, University of Western Australia, WA 6009, Australia

ARTICLE INFO

Article history:
Received 24 July 2007
Received in revised form 23 July 2008
Accepted 10 September 2008
Available online 1 October 2008

Keywords:
Folding
Non-equilibrium thermodynamics
Thermal–mechanical feedback

ABSTRACT

Folding of viscous layered rocks is traditionally viewed as an instability arising from viscosity differences between layers. This approach derives from Biot, and for purely viscous materials predicts the growth of single wavelength systems; the dominant wavelength is sensitive to layer thickness, the viscosity ratio between the layers, the amount of shortening and the boundary conditions. This paper presents one alternative theory of folding to that of Biot and addresses the deformation of elastic-viscous materials where the viscosity ratio between layers is small and Biot theory predicts folds will not form. Such ratios are consistent with situations in the mid to lower crust as indicated by experimental data. Folding results from the coupling between temperature dependent viscosity and heat generated by deformation; the result is weakening in the hinges of embryonic folds and subsequent buckling. This process is distinct from the Biot buckling process. The structures that develop resemble natural structures in that folds develop at a range of length scales, hinges undergo strong thickening, and axial plane crenulations form. This approach is grounded in non-equilibrium thermodynamics; the coupling of deformation to fluid flow and chemical reactions is explored as part of a unified framework for rock deformation processes.

1. Introduction

1.1. Background

The formation of folds in deformed rocks is traditionally considered in terms of contrasts in competency between layers (e.g. Ramberg, 1963; Biot, 1965; Sherwin and Chapple, 1968; Smith, 1975, 1977; Johnson and Fletcher, 1994). We use the term *competency contrast* to mean differences in the rheological properties of rocks whether these rheological properties are the elastic moduli, plastic properties such as cohesion or friction angle, or viscous properties such as the effective viscosity of power law viscous materials (see Section 3). Although there have been considerable advances in identifying specific constitutive relations operating during rock deformation, the term competency is still useful as a general term for the field geologist who remains uncertain as to which constitutive relation is relevant for field examples. All of these properties are measures of how much stress a material can maintain for given imposed deformation conditions and Biot (1965) together with subsequent workers (Sherwin and Chapple, 1968; Fletcher, 1974; Smith, 1975, 1977, 1979; Johnson and Fletcher, 1994) have shown that strong differences in all of these properties contribute to the amplification of folding instabilities. The basis of the traditional theory is that the deformation of layered rocks is intrinsically unstable, given enough competency contrast between the layers, so that perturbations in the geometry of the layers are amplified by the deformation as the result of local perturbations induced in the imposed velocity field (Fletcher, 1974; Cobbold, 1975, 1976; Smith, 1975, 1977, 1979; Fullagar, 1980). For some combinations of rheological parameters this inhomogeneous velocity field amplifies initial heterogeneities with continuing deformation and folds develop.

For shortening deformations of layered linear viscous (Newtonian) materials, with large (>100) ratios between the viscosities of the layers and driven by a constant force parallel to the layer, a single wavelength grows faster than all others leading to a dominant wavelength for folds known as the Biot dominant wavelength, λ_B. For large viscosity ratios the ratio of λ_B to the layer thickness is much greater than the wavelength to thickness observed in naturally deformed rocks and Sherwin and Chapple (1968) showed that for this particular constitutive relation and boundary conditions, folds with naturally observed wavelength to thickness ratios (4–7, and hence less than λ_B) can develop at realistic shortening strains (40%) and low viscosity ratios of 18–20 if layer parallel shortening is taken into account. For viscosity ratios <10 the amplification is small so that no folds develop. The wavelength of folding that develops in a particular situation is the dominant wavelength, λ_D, also called the preferred wavelength (Johnson and Fletcher, 1994), and this is usually less than λ_B.

* Corresponding author. CSIRO Exploration and Mining, P.O. Box 1130, Bentley, WA 6102, Australia. Tel.: +61 418 395 545.
E-mail address: bruce.hobbs@csiro.au (B. Hobbs).

0191-8141/$ – see front matter © 2008 Published by Elsevier Ltd.
doi:10.1016/j.jsg.2008.09.002

For a linear theory of folding of viscous materials (Biot, 1965; Johnson and Fletcher, 1994) similar results to those of Sherwin and Chapple hold for constant strain rate or velocity boundary conditions (Johnson and Fletcher, 1994). However for a non-linear theory where the kinematic constraints of constant velocity or constant strain rate are taken into account (Mühlhaus et al., 1994), the results resemble those of Sherwin and Chapple (1968) except that the amplification is significantly smaller for a given viscosity ratio to the extent that significant amplification does not develop unless the viscosity ratio is of the order of 50. For this viscosity ratio the initial dominant wavelength is λ_B but this decreases as shortening proceeds. For viscosity ratios less than approximately 50, the perturbation field remains small or decays in importance with increasing strain and the embedded layer mainly thickens homogeneously with only small amplitude folding deflections developing. For viscosity ratios less than 10, no folds develop. In contrast to the Sherwin and Chapple result, folds with $\lambda_D < \lambda_B$ develop for large viscosity ratios. Experimental data indicate that viscosity ratios as small as 2–5 may be common in the mid to lower crust so that the development of folds by a process other than the Biot process must be considered.

In this paper we explore one mechanism alternative to that of Biot for the formation of folds in which the feedback between the heat generated by deformation results in shear zones within which there is a localised weakening of the rock. We emphasise that quite small fluctuations in temperature (of the order of 2–10 °C) above ambient temperature are sufficient to generate the effects we describe here. Intersection of these shear zones with layers leads to weakened embryonic hinges that buckle and then amplify to produce the observed structures. This thermal–mechanical approach leads to folding with small viscosity ratios (<10) and low values of the stress exponent, N (<5), for power-law materials, consistent with the mechanical properties inferred from experimental data.

The basic approach adopted in this paper derives from the non-equilibrium thermodynamic theory of coupled, deforming systems. The term *coupled* is meant to imply that during deformation two or more processes operate that have strong feedback influences on each other. In particular the dissipation of energy is considered as a basic feedback process. By *dissipation* we mean the conversion of energy generated by mechanical, chemical or other processes into heat or sound and the conduction of this heat within or out of the system. In this paper we concentrate solely upon the influence of heat generated by mechanical dissipation on the development of folds in layered materials. Preliminary results have been published in Hobbs et al. (2007).

1.2. Purpose of the paper

The purpose of this paper is to explore mechanisms of folding that derive from the coupling of two or more processes such as thermal–mechanical, fluid–mechanical or chemical-mechanical coupled feedback interactions, but with an emphasis on thermal–mechanical coupling. The importance of coupling two or more processes together lies in the emergence of new phenomena that do not arise in the un-coupled system. These new phenomena comprise instabilities, such as the localisation of deformation into shear zones and the amplification of perturbations to produce folds and boudinage; it is to be emphasised that such instabilities do not occur in many of the systems explored here with realistic geological parameters unless the processes are coupled. In this paper we explore the development of folds; another paper (Hobbs et al., submitted) considers the development of boudinage.

This coupled approach incorporates detailed mechanisms of deformation that are not present in classical theories of folding. In turn, this introduces a very large range of length scales for folding and boudinage together with geometries that are not intrinsically periodic. Surprising results also emerge in that differences in properties other than mechanical properties (such as viscosity) can lead to fold amplification. Such situations involve differences in thermal softening (in thermal–mechanical systems driven by differences in the activation enthalpy), differences in dilatancy (in fluid–mechanical systems) and differences in chemical potential (in chemical-mechanical systems). Perhaps of even greater interest is the emergence of a range of other structures as a natural consequence of the coupling. These structures include axial plane cleavages and schistosities, crenulation cleavages, lineations, porphyroblasts, metamorphic differentiation and various vein and fracture systems, all of which are intrinsically associated with the folding of layered sequences in natural examples.

The coupled approach explored here integrates concepts of fold development across a range of length scales as well as placing the development of other fabrics commonly observed in association with natural folds, within a unified framework. Within this framework, the classical un-coupled Biot approach appears as a special case that arises for relatively low temperatures and fast strain rates and where thermal, fluid, chemical, damage and fabric-evolution feedback coupling relations are not considered. Our proposal in this paper is that the incorporation of such effects is not only realistic, but also introduces an extremely rich array of behaviours that form an integrated conceptual package that sheds light on the development of deformed metamorphic rocks. The study of coupled systems involves examining systems far from equilibrium where in addition to the conventional continuity and momentum equations, the energy fluxes in the system arising from deformation, fluid flow, thermal transport and chemical reactions/transport, are tracked and the feedbacks between energy dissipation and the constitutive behaviour are addressed. Such processes are constrained by the Second Law of Thermodynamics as expressed by the Clausius–Duhem Inequality (Truesdell and Noll, 1965, section 79). The fundamental concepts are not necessarily associated with heat generated by deformation and thermal feedback. The basic driver is the tendency for non steady state systems to evolve so that entropy production is maximised subject to the constraints imposed (Ziegler, 1983; Martyushev and Seleznev, 2006) so that even in temperature insensitive materials, such as Mohr-Coulomb materials, the same formalism and effects apply (Collins, 2003).

1.3. Plan of the paper

The traditional approach to folding in uncoupled systems is from a non-thermodynamic point of view and is the pathway followed by most workers since Biot (Ramberg, 1963; Fletcher, 1974, 1991; Smith, 1975, 1977, 1979; Johnson and Fletcher, 1994) so that it is not commonly appreciated in the geological literature that Biot had an equivalent but alternative path to folding theory based on non-equilibrium thermodynamics (Biot,1984). In Section 2 we follow the non-thermodynamic path to set the boundaries for applicability of the non-coupled theories and to illustrate the controls of boundary conditions and constitutive parameters on amplification factors and wavelengths that develop. In Section 3 we briefly review the experimental work on the competency differences that exist in rocks and point out that differences in any mechanical property as large as 100 are probably rare, as are values of N greater than 5, except in the topmost crust, and even then for special rock assemblages. For conditions corresponding to the mid to lower crust viscosity ratios as high as 20 would seem to be rare so that it becomes difficult to explain the development of natural folds in the mid to lower crust using the traditional theories. In Sections 4 and 5 we specifically develop the non-equilibrium thermodynamic theory of deforming materials with thermal feedback and then in

Section 6 apply this theory to the development of folds in single and multi-layered systems. These results are compatible with what is observed in naturally deformed rocks from the point of view that the fold profiles are less regular than predicted by the uncoupled theory, scale invariance emerges naturally so that folds appear at many length scales, the wavelength to thickness ratios are small (2 to 4) and hence less than λ_B, and fold profiles range from Type 1A to Type 3 of Ramsay (1967) rather than being more or less concentric as expected from the un-coupled theories (e.g. Schmalholz et al., 2001). In Section 7 we emphasise that the thermal–mechanical approach adopted here is but one avenue leading to an understanding of the folding of layered, coupled systems and that damage, microstructural, chemical and fluid flow processes result in similar structures but at different length scales and in differing geological environments. We draw this to a conclusion in Section 8. Mathematical symbols are defined as they are introduced and also in Table 1.

2. Deformation with no thermal feedback

2.1. The stability of deforming systems

This paper is concerned with the conditions under which a deforming system becomes unstable through feedback relations between mechanical behaviour and thermal, fluid, and chemical transport processes. There are two fundamental ways in which such instability can occur. One consists of the growth of perturbations in an initially homogeneous system and the other consists of a bifurcation in behaviour, or the spontaneous development, and subsequent growth of one out of two new evolutionary paths, for the system. The classical Biot approach is concerned with the first of these instability types; the feedback processes discussed here are concerned with the second type.

For shortening at constant force of a system consisting of geometrical perturbations of a highly viscous layer embedded in a low viscosity matrix, Biot (1965) showed that one wavelength of perturbation, λ_B, given by equation (1) below, grows preferentially and at an exponential rate; all other perturbations grow relatively slowly. This system is unstable with respect to perturbations of wavelength, λ_B, and the instability exists from the instant deformation begins. The results of the linear theory developed by Biot describe what happens during a small deformation after instability develops. Such an evolution may continue to larger deformations or other evolutionary trends may develop (Mühlhaus et al., 1994). Examples of bifurcation behaviour include the development of shear bands in hitherto homogeneously deforming material and the development of chemical differentiation in material of hitherto homogeneous chemical composition.

These two types of instability can be closely associated in some materials in that the bifurcation event can generate new perturbations that are then amplified. However both types of instability do not occur in all materials. Thus, bifurcation, leading to shear localisation, does not occur in an isotropic, viscous (including power law) material with no softening (Anand et al., 1987) whereas growth of perturbations does occur. Both types of behaviour occur in Mohr–Coulomb plastic materials and in anisotropic viscous materials (Hobbs et al., 1990, 2000; Mühlhaus et al., 2002).

2.2. Classical un-coupled folding theory

The classical un-coupled treatments of buckling of elastic, plastic or viscous single layers embedded in another medium originated with Biot (1937, 1957, 1959, 1961, 1963, 1965); identical developments were made by Ramberg (1963) for viscous materials. The common result of all such treatments, if the layer or the embedding materials are elastic, linearly viscous or power

Table 1
Symbols used in this paper, units and typical values

Quantity	Description	Units, typical values
A	Pre-exponential factor	$Pa^{-N} s^{-1}$
c	Cohesion	Pa
c_p	Specific heat at constant pressure	1450 J kg^{-1} K^{-1}
D	Deformation rate	s^{-1}
D/Dt	Material time derivative	
d	Grain size	μm
d_o	Reference grain size	1μm
E	Young's modulus	4.5×10^9 Pa
E_L	Young's modulus for layer	Pa
E_e	Young's modulus for embedding medium	Pa
e	Specific internal energy	J kg^{-1}
f	Body force	N
h	Thickness of layer	m
J_2	Second invariant of the deviatoric stress	Pa^2
J_K	Mass flux of Kth chemical component	kg m^{-2} s^{-1}
k	Shear zone thickness	m
L	Length after deformation or length scale	m
L_0	Length before deformation	m
l_{therm}	Thermal diffusion length scale	m
m	Mass	kg
m_K	Mass of Kth chemical component	kg
N	Stress power law exponent	Dimensionless
N_L	Stress power law exponent for layer	Dimensionless
N_e	Stress power law exponent for embedding medium	Dimensionless
n	An integer	Dimensionless
P	Axial force	N
$Pe^{thermal}$	Thermal Peclet number	Dimensionless
p	Confining pressure	Pa
p_f	Fluid pressure	Pa
Q	Activation enthalpy	J mol^{-1}
q	Heat flux	J m^{-2}
R	Gas constant	8.3143 J K^{-1} mol^{-1}
r	Heat supply per unit mass	J kg^{-1}
s	Specific entropy	J kg^{-1} K^{-1}
T	Absolute temperature	K
T_c	Critical temperature where thermal–mechanical feedback becomes important	K
t	Time	s
$\tilde{t}$	Dimensionless time	Dimensionless
u	Local material velocity vector	m s^{-1}
w	Sideways deflections of a layer	m
w_o	Initial perturbation of layer	m
w_n	Deflection associated with mode n	m
x_i	Spatial coordinates	m
α	Volumetric expansion coefficient	3.1×10^{-5} K^{-1}
α_{ij}	Volumetric expansion tensor	K^{-1}
α_i	Collection of scalar, vector and tensor internal state variables	Units of relevant scalars, vectors or tensors
δ	Grain size exponent	Dimensionless
ε_{ij}	Strain tensor	Dimensionless
$\dot{\varepsilon}_{ij}$	Strain-rate tensor	s^{-1}
ζ	Variation in fluid content in a porous system	Dimensionless
η	Viscosity	Pa s
η_L	Viscosity of layer	Pa s
η_e	Viscosity of embedding medium	Pa s
κ	Thermal diffusivity	0.6×10^{-6} m^2 s^{-1}
Λ	Normalised axial force	Dimensionless
λ_B	Biot dominant wavelength	m
λ_D	Dominant or preferred wavelength	m
μ	Elastic shear modulus	Pa
μ_K	Specific chemical potential of Kth chemical component	J kg^{-1}
ν	Poisson's ratio	0.3 Dimensionless
ρ	Mass density	2750 kg m^{-3}
σ_{ij}	Cauchy stress tensor	Pa
σ'_{ij}	Deviatoric stress tensor	Pa
$\overset{\nabla}{\sigma}_{ij}$	Objective corotational stress tensor	Pa
τ	Yield stress	Pa
v_k	Array of k scalar, vector and tensor internal state variables	Units of relevant scalars, vectors or tensors
Φ	Dissipation function	J kg^{-1} s^{-1}
Φ^s	Specific dissipation	J kg^{-1} s^{-1}
$\Phi^{chemical}$	Chemical dissipation	J kg^{-1} s^{-1}

Table 1 (*continued*)

Quantity	Description	Units, typical values
φ	Friction angle	Degrees
χ	Thermal efficiency	Dimensionless
Ψ	Specific Helmholtz Free Energy	J kg^{-1}
ω	Amplification factor	Dimensionless
ω_T	Total normalised growth rate	s^{-1}

law-viscous is that just one particular wavelength (the dominant wavelength) is amplified. For elastic-viscous materials a range of other fold geometries is possible ranging from single wavelength fold trains to two wavelength geometries to fold systems with spatially decaying amplitudes (Mühlhaus et al., 1998; Jeng et al., 2002; Jeng and Huang, 2008), to the development of localised fold packets (Hunt et al., 1996b) and to fractal geometries (Hunt et al., 1996a). However for purely viscous materials, periodic fold geometries result from the classical theories no matter what boundary conditions, initial geometry or initial deviations from the ideal planar state exist. Mancktelow (1999, 2001) has explored the influence of various forms of initial geometrical perturbations on fold growth and has shown that initial probability distributions do not have an appreciable influence upon the wavelengths of folds although they do impact on the amount of layer shortening during folding.

2.2.1. Definition of the deforming system

The problem is usually set up as shown in Fig. 1. A single thin layer of thickness, h, is embedded in a less competent medium and the whole assembly is subjected to constant force, stress, velocity or strain rate boundary conditions resulting in shortening in the direction parallel to the initial orientation of the layer (x_1). The constitutive parameters for the layer are the Young's Modulus, E_L, the elastic shear modulus, μ_L, the effective viscosity, η_L, and the power law exponent, N_L. Similarly, for the embedding medium, these parameters are E_e, μ_e, η_e and N_e respectively. The response of this system is quite sensitive to the boundary conditions. This arises because the amplification rate of folding depends on the force, P, parallel to x_1 (Biot, 1965; Mühlhaus et al., 1994). For constant stress boundary conditions, P must increase as the thickness increases so that amplification is faster than for constant P conditions. For constant velocity boundary conditions the boundary cannot accelerate and so P decreases with time as does the amplification rate. For constant strain rate conditions, the velocity decreases with time. Thus the amplification rates for constant strain rate conditions are less than for constant velocity conditions. For small shortening strains, the realm of the Biot theory, all of these boundary conditions give the same result. Except for Mühlhaus (1993) and Mühlhaus et al. (1994) these dynamic and kinematic constraints have not been considered in the literature.

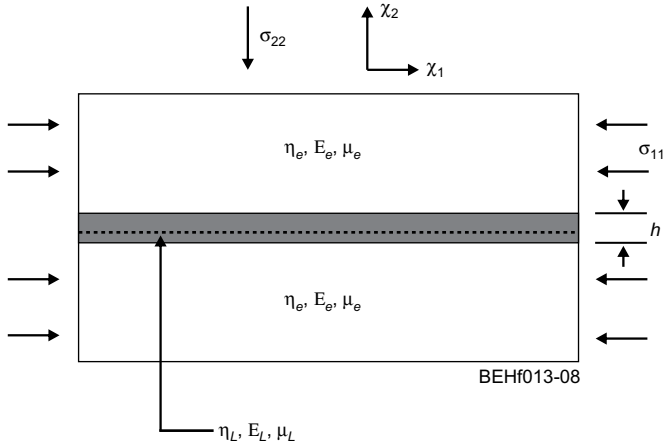

Fig. 1. Model set-up. A single layer of thickness, h, and with Young's Modulus, E_L, elastic shear modulus, μ_L, and effective viscosity (given by equation (10)), η_L, is embedded in a medium with Young's Modulus E_e, elastic shear modulus μ_e and viscosity, η_e. The assembly is shortened in the x_1 direction by an imposed stress, σ_1, force, P, velocity or strain-rate. For power-law viscous materials the stress exponents N_L and N_e also need to be explicitly considered.

2.2.2. Deformation of viscous materials

As an example, for a linear viscous constitutive law, the Biot dominant wavelength, is given by

$$\lambda_B = 2\pi h \sqrt[3]{\frac{\eta_L}{6\eta_e}} \tag{1}$$

Thus for a value of 6000 for η_L/η_e one expects a dominant wavelength of approximately 63 times the layer thickness. One should note that typical values of λ/h for real rocks are in a narrow range of 2–7 (see Sherwin and Chapple, 1968; Smith, 1979; Price and Cosgrove, 1990; Johnson and Fletcher, 1994; Patton and Watkinson, 2005 for reviews). Thus, for natural ranges of λ/h equation (1) predicts viscosity ratios of 0.2–8.3 for naturally deformed rocks if they were composed of linear viscous materials.

For linear viscous materials with constant stress boundary conditions, the normalised growth rate, ω_T, which is the growth rate of perturbations divided by the background strain-rate, is defined by (Smith, 1975)

$$\ln\frac{w}{w_o} = -\omega_T \ln\frac{L}{L_o} \tag{2}$$

where w_o, w are the initial and current amplitudes of the perturbations and L_o, L are the initial and current lengths of a line initially parallel to the undeformed layer. Thus if $\omega_T = 5$, shortening of 50% produces an amplification of $w/w_o = 32$.

The magnitude of the total normalised growth rate, $|\omega_T|$, corresponding to the dominant wavelength for constant applied force in Newtonian viscous materials is (Biot, 1961; Smith, 1975)

$$|\omega_T| = \left(\frac{4\eta_L}{3\eta_e}\right)^{2/3} + 1 \tag{3}$$

Non-linear viscous layered materials behave in much the same manner as Newtonian materials (see Fletcher, 1974; Smith, 1977, 1979) except that the growth rates are commonly larger and the dominant wavelengths smaller than for linear materials. The expression equivalent to equation (1) for power-law materials is

$$\lambda_D = 2\pi h \sqrt[3]{\frac{\eta_L N_e^{0.5}}{6\eta_e N_L}} \tag{4}$$

where λ_D is the dominant wavelength. If $N_L > \sqrt{N_e}$, the dominant wavelength for power law materials is less than that for Newtonian materials. Equation (4) is an asymptotic expression for $\eta_L/\eta_e >$ ca. 50. For small values of η_L/η_e (less than say 10) λ_D is nearly constant and lies in the range 4 to 6 for a wide range of stress exponent values (Smith, 1977).

The total normalised fold amplification rate for power law viscous materials (Smith, 1977) is

$$|\omega_T| = \left(\frac{4\eta_L}{3\eta_e}\right)^{\frac{2}{3}} (N_L N_e)^{\frac{1}{3}} + 1 \tag{5}$$

This again is an asymptotic expression approximately true for values of $\eta_L/\eta_e > 20$. For values of $\eta_L/\eta_e < 10$ and for N_L and $N_e < 5$, $|\omega_T|$ is less than about 8 and for $\eta_L/\eta_e < 5$, $|\omega_T|$is less than 2. Thus

although power law constitutive relations predict realistic dominant wavelengths, the growth rates corresponding to these realistic values are too small to produce geologically realistic folds.

In the studies discussed above, the layer is compressed with a constant force, P, parallel to x_1. As discussed above, the results that are derived from such a model can be quite different to those that arise if the boundary conditions consist of a constant velocity or strain rate parallel to x_1 and one considers large deformations. The following important points that are different to the classical Biot results need to be noted.

For a Newtonian viscous layer embedded in a less viscous medium with constant force boundary conditions a dominant wavelength is exponentially amplified (accompanied by exponential growth in the shortening strain rate) and the wavelength is a function of both the viscosity ratio and the amount of shortening parallel to x_1 (Sherwin and Chapple, 1968). As we have noted, Sherwin and Chapple (1968) show that for relatively small viscosity ratios of 18–20, wavelength to thickness ratios of 5–7 can be developed for 40% shortening. This compares favourably with observations of natural folds under the assumption that the boundary conditions in Nature consist of constant imposed force. For viscosity ratios <10 amplification is small and no folds develop.

The linear theory for constant velocity or strain rate boundary conditions gives similar results to those of Sherwin and Chapple (Johnson and Fletcher, 1994). However, if non-linear effects are taken into account, constant velocity or strain rate boundary conditions do not lead to the same results as constant force boundary conditions (Mühlhaus et al., 1994). For constant velocity conditions the force in the layer decreases, as does the fold growth rate, with increasing shortening. This evolution of force is shown in Fig. 2a, modified from Mühlhaus et al. (1994). Fig. 2b and c show the evolution of amplification with increasing time for various normalised wavelengths. For small deformations (the regime relevant for the linear stability analysis and the linear theories), the Biot dominant wavelength is the fastest growing mode but very quickly with continued shortening, shorter wavelengths grow faster. The growth of the Biot wavelength is exponential according to the linear theory but if kinematic constraints are taken into account, the growth rate of all wavelengths is monotonically decreasing although growth rates for shorter wavelengths decrease fastest. However, in general, the longer wavelength modes have the smallest total amplification and only the shortest wavelengths ($\lambda_D < \lambda_B$) have significant total amplifications. Thus these shorter wavelength modes dominate especially as the viscosity ratio becomes large (say >100).

In some respects, this result is similar to the result of Sherwin and Chapple in that wavelength to thickness ratios smaller than the Biot dominant ratio ultimately dominate but in this case the amplification rate is no longer exponential and rapidly decays so that, except for large viscosity ratios, the layer essentially shortens homogeneously with little fold growth. Thus the results of Mühlhaus et al. (1994) indicate that for a viscosity ratio of 20, λ_B is the dominant mode up to 50% shortening, the maximum amplification being negligible at about 5 (Fig. 2c). In contrast to the situation for constant force boundary conditions, high viscosity ratios with constant velocity boundary conditions produce very short wavelength folds. Thus a viscosity ratio of 3000 results in modes equivalent to $0.1\lambda_B$ developing for most of the folding history (Mühlhaus et al., 1994 and Fig. 2b) with a maximum amplification at 50% shortening of about 150. Constant stress boundary conditions would lead to a mode approximately equal to λ_B developing (Sherwin and Chapple, 1968, their Fig. 3). The results of Mühlhaus et al. (1994) need to be modified in that they do not consider the influence of continued shortening after the amplification rate becomes small. This results in further reduction in λ_D as is discussed below in Section 2.2.4 and is similar to the Sherwin and Chapple effect.

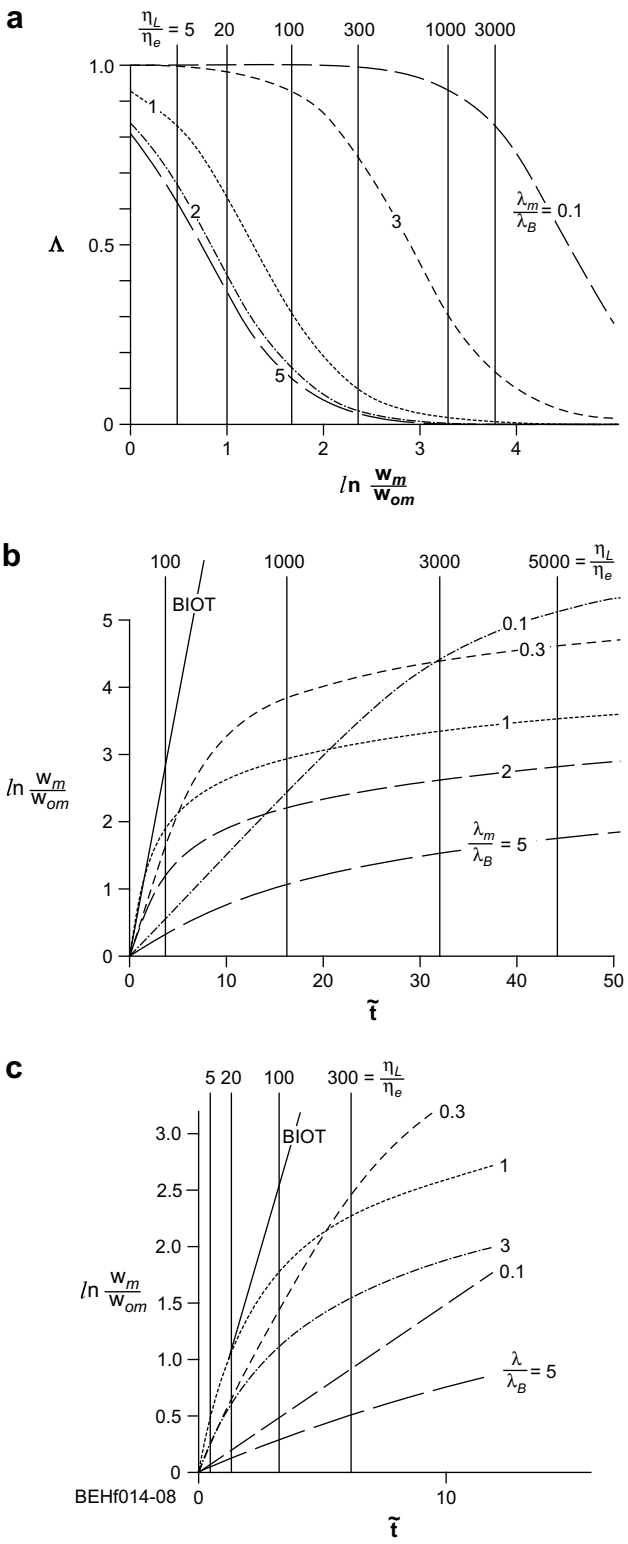

Fig. 2. Behaviour of viscous layered material embedded in viscous material with constant velocity boundary conditions (after Mühlhaus et al., 1994). (a) Evolution of the normalised axial force, Λ, in the layer with amplification for various λ_m/λ_B. w_m is the displacement associated with wave number, m, and w_{om} is the initial perturbation associated with that mode. The calculations are made for $w_{om}/h = 0.1$. The figure plots results for values of λ_m/λ_B ranging from 5 to 0.1. (b) Evolution of amplitude, w_m/w_{om}, with dimensionless time, $\bar{t}$ where $\bar{t} = \varepsilon(\eta_L/\eta_e)^{\frac{1}{3}}$ and ε is the shortening strain. Values of $\bar{t}$ at 50% shortening strain for values of η_L/η_e of 10^2, 10^3, 3×10^3 and 5×10^3 are shown as well as results from the linear stability analysis (Biot). (c) Zoom into Fig. 3(b) showing values of $\bar{t}$ at 50% shortening strain for values of η_L/η_e of 5, 20, 10^2 and 3×10^2.

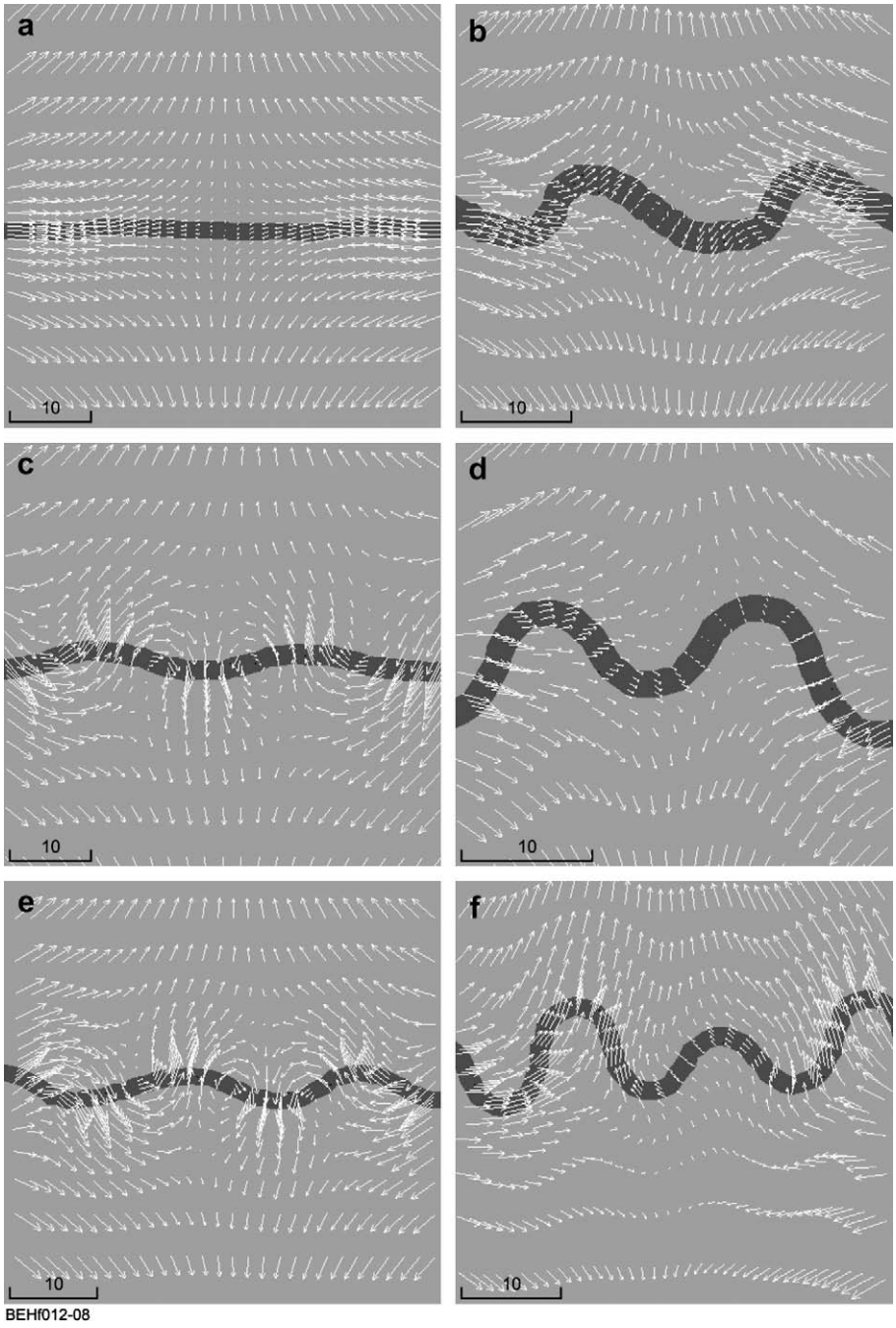

Fig. 3. Perturbation velocity field in elastic-Newtonian viscous materials for various viscosity ratios. Shortening strain-rate = 10^{-12} s^{-1}. Viscosity of the embedding material is always 10^{19} Pa s. (a) η_L/η_e = viscosity ratio = 20, shortening = 11%. Perturbation field reinforces the imposed homogeneous velocity field; weak deflections correspond to $\lambda_D = 1.7\lambda_B$, $\lambda_D/h = 15$; (b) Viscosity ratio = 20, shortening = 40%, $\lambda_D = 1.4\lambda_B$, $\lambda_D/h = 13.5$. Perturbation field has evolved to almost homogeneous shortening. (c) Viscosity ratio = 200, shortening = 11%. Perturbation field drives the development of antiforms and synforms; $\lambda_D = 0.6\lambda_B$, $\lambda_D/h = 10$ (d) Viscosity ratio = 200, shortening = 40%. Perturbation field has evolved to almost homogeneous shortening; $\lambda_D = 0.4\lambda_B$, $\lambda_D/h = 7$. (e) Viscosity ratio = 3000, shortening = 11%. Perturbation field now very strong; $\lambda_D = 0.3\lambda_B$, $\lambda_D/h = 12$. (f) Viscosity ratio = 3000, shortening = 40%. Perturbation field has evolved to almost homogeneous shortening; $\lambda_D = 0.2\lambda_B$, $\lambda_D/h = 8$.

These results have important implications for the interpretation of natural folds under the assumption that the materials involved behave as viscous materials with no elasticity. Thus a fold system with wavelength to thickness ratios in the range 5–7 with an assumed amplification of 100 and a shortening of 50% would be interpreted as having viscosity ratios of approximately 20 under the Sherwin and Chapple analysis with constant force boundary conditions. For the Mühlhaus et al analysis for constant velocity boundary conditions this same fold system with the same assumptions of amplification and shortening corresponds to a viscosity ratio of approximately 3000 with $\lambda_D = 0.1\lambda_B$.

2.2.3. Deformation of elastic-viscous materials

The inclusion of elasticity in the material constitutive relations, together with viscosity, adds considerable complexity, so much so that a general theory of folding of layered elastic-viscous materials is in its infancy (Hunt et al., 1996b). The theory of folding of layered viscous materials as developed by a host of workers (Biot, 1965; Fletcher, 1974; Smith, 1975; Johnson and Fletcher, 1994) is essentially a linear theory where the evolution of the system is described by a differential equation with fourth order spatial derivatives. Such equations are readily interpreted in terms of harmonic solutions which may be expanded as Fourier series in which the growth of

each wavelength is independent of all others. This leads immediately to the study of dispersion relations and an emphasis on the identification of the fastest growing, or dominant, wavelength.

For elastic-viscous materials the differential equation describing the evolution of the system is still fourth order in spatial derivatives but also involve time. Now the opportunity exists for interference between modes and non-harmonic solutions or localisation of folding may arise. In this case the concept of a dominant wavelength may no longer be relevant and a host of different waveforms are possible including the development of localised wave packets (Hunt et al., 1996a).

The behaviour of the material now becomes strain rate dependent (Hunt et al., 1996b; Schmalholz and Podladchikov, 1999; Zhang et al., 2000; Jeng and Huang, 2008). For fast strain rates the material may behave as an elastic material and the kink folds and localised fold packets described by Hunt and co-workers (Hunt et al., 2000, 2001) arise. This behaviour represents another kind of non-Biot folding mechanism (other than the coupled feedback mechanisms discussed in this paper) and is undoubtedly important in the upper crust of the Earth.

For a Maxwell elastic-viscous material the response of a layer subjected to a deformation rate parallel to x_1 of D is given by

$$\frac{\dot{P}}{4\mu}+\frac{P}{4\eta}+hD = const. \tag{6}$$

(Jaeger, 1969; Mühlhaus et al., 1994, 1998) where P is the force parallel to x_1 in the layer. If constant force boundary conditions are adopted this behaves as a purely viscous material so that one expects the same results as found by Sherwin and Chapple although the wavelength may be dependent on the magnitude of the compressive force (Biot, 1957). However for constant velocity or strain rate conditions this kinematic constraint implies that P is no longer constant and is a function of time, t, with $\dot{P} \leq 0$. Thus the behaviour of a Maxwell material with constant velocity or strain rate boundary conditions is qualitatively similar to that of a purely viscous material with the same boundary conditions and so similar to the behaviour described by Mühlhaus et al. (1994) and summarised in Fig. 2.

The paper by Neurath and Smith (1982) purports to present experimental evidence that folds can develop with viscosity ratios as low as 7.3. The materials involved are modelled as viscous power law materials with no elasticity even though the stress strain curves exhibit linear pre-yield segments with an apparent elastic modulus, μ, of approximately 4×10^6 Pa. The material comprising the embedded layer (microcrystalline wax) is clearly elastic-viscous and apparently exhibits strain softening. The boundary conditions consist of constant imposed velocity so that the discussion presented by Mühlhaus et al. (1994) is pertinent. The two strain rates investigated ($0.29 \times 10^{-4}\,s^{-1}$ and $1.1 \times 10^{-4}\,s^{-1}$) correspond to viscosities of 2×10^8 Pa s and 8×10^6 Pa s respectively resulting in very small relaxation times (ratio of viscosity to shear modulus) for the layer of 50 s and 2 s respectively. The decrease in amplification rate with continued deformation demonstrated experimentally by Neurath and Smith (1982) is in keeping with a relaxation in stress in the layer as expected from the boundary conditions and the constitutive properties. Note that the straight grid lines initially marked on the Neurath and Smith specimens show little distortion even when they are within one layer thickness of the deflections shown by the layer. The specimens are initially shaped so that the predetermined dominant wavelength is prescribed as deflections before deformation begins and these distortions remain and grow somewhat during subsequent deformation. The lack of folding distortions of the grid lines close to the layer shows that deformation is nearly homogeneous. Most of the deformation recorded in these specimens consists of passive amplification of initially prescribed perturbations with little or no folding. This same decrease in amplification rate has been recorded in numerical experiments by Zhang et al. (1996) and is consistent with the analysis of Mühlhaus et al. (1994).

2.2.4. The dominant wavelength in elastic-viscous materials; constant strain rate conditions

The discussion of fold wavelength evolution given by Mühlhaus et al. (1994) applies to a purely viscous material embedded in another purely viscous material. If the strain rate is small enough, (Hunt et al., 1996b; Schmalholz and Podladchikov, 1999; Zhang et al., 2000; Jeng and Huang, 2008) a Maxwell elastic-viscous material behaves as a viscous material. In Fig. 3 the behaviour of a Maxwell material embedded in another Maxwell material is explored for constant strain rate boundary conditions and a range of viscosity ratios. The imposed strain rate is small enough that the materials behave as viscous materials. The behaviour follows that illustrated in Fig. 2 for low shortening strains but as the shortening strain increases and the amplification rate for a particular wavelength decreases to low values the layered material undergoes almost homogeneous pure shearing and the wavelength established early in the history undergoes shortening in much the same way as proposed by Sherwin and Chapple (1968) for constant force boundary conditions. Thus there are two processes operating to establish the dominant wavelength, one is the process of continuous evolution to smaller wavelengths described by Mühlhaus et al. (1994) and superimposed on this is a Sherwin and Chapple type of process which leads to homogeneous shortening of previously established wavelengths.

The initial geometry for Fig. 3 is given in Fig. 1 and the constitutive relation is elastic-linear viscous (Maxwell coupling) with elastic constitutive parameters given in Table 4. The viscosity ratios are given in the figure caption and below. The layer has been initially distorted according to a perturbation field given by

$$w = w_o \sum_{n=1}^{10} \sin\frac{10x_1}{n\lambda_B}$$

where $w_o = 0.05h$. A sensitivity analysis such as illustrated in Fig. 3 shows that folding does not begin to become important at shortening strains of 40% until viscosity ratios reach approximately 50. At viscosity ratios of 10 and shortening strains of 40% low amplitude deflections develop. One needs to adopt far larger viscosity ratios for significant folding to be established by reasonable (say 30%) total shortening. At viscosity ratios less than 50, the initial perturbation velocity field predicted by the linear theories decays with increased strain to ultimately simply reinforce the imposed homogeneous strain field. In keeping with the analysis of Mühlhaus et al. (1994) and summarised in Fig. 2, $\lambda_D < \lambda_B$ especially at large viscosity ratios but by 40% shortening the ratios of dominant wavelength to thickness for viscosity ratios less than about 1000 are still above or near the upper limits of what are observed in natural examples. The examples in Fig. 3 result from a bulk shortening strain rate of $10^{-12}\,s^{-1}$. The same general behaviour is observed at a strain rate of $10^{-13}\,s^{-1}$.

Natural folds are rarely, if ever, strictly periodic; that is they are rarely characterised by a single dominant wavelength or a narrow distribution around a dominant wavelength. A clear example here is the ubiquitous existence in Nature of parasitic folds. The situation is not resolved by introducing geometrical non-linearities such as initial irregularities (see Abbassi and Mancktelow, 1990, 1992; Mancktelow, 1999, 2001). One may propose that non-linear constitutive laws will solve the problem. However power-law viscous materials give similar results to linear viscous materials (Fletcher, 1974; Smith, 1977, 1979; Mühlhaus et al., 1998) except the dominant wavelength, as noted above, is less than λ_B. In some

instances, for elastic-viscous materials, two wavelengths do develop (Mühlhaus et al., 1998; Jeng et al., 2002; Jeng and Huang, 2008). The discussion of Mühlhaus et al. (1998) indicates that for the development of two wavelengths in layered Maxwell materials with realistic relaxation times and strain rates, the viscosity ratios need to be large (>1000). Localised wave packets can develop if there is a significant contribution from elastic behaviour (Hunt et al., 1996a). Patton and Watkinson (2005) used a Second Order Fluid and predict folds with λ/h ratios in the range 2–7 with low viscosity ratios but a single wavelength is amplified.

Thus, the classical Biot approach, and its extension to non-linear viscous materials, is capable of qualitatively explaining the basic geometrical features of folds, namely periodicity and a wavelength proportional to layer thickness. Non-linear viscous materials do produce realistic dominant wavelengths but only for unrealistic stress exponents involving N greater than about 5. Exponents as large as this are rare in experimental results (marble, with $N = 7$–8, is the exception, Heard and Raleigh, 1972; Walker et al., 1990). This prompted the suggestion (Fletcher, 1974; Smith, 1975, 1977) that experimental results may not be representative of natural deformation conditions. This issue remains open. Linear viscous materials predict dominant wavelengths that are comparable to natural situations for realistic growth rates for constant force boundary conditions for viscosity ratios as low as 20 if layer parallel shortening is taken into account but for constant velocity and strain rate conditions amplification rates are relatively small and realistic folds do not develop unless viscosity ratios are of the order of 3000. Elastic-viscous materials with constant force boundary conditions behave as viscous materials but constant strain rate conditions again result in folding only for large (>50) viscosity ratios.

3. Mechanical differences in natural materials

Since, in the classical theories, the folding instability arises from differences in competency, we explore in this section the ranges of differences that are likely to exist in rocks given the experimental data available.

3.1. Elasticity

Data for elastic moduli of rocks are given in Table 2. Two elastic moduli are required to define the elasticity of an isotropic medium (see Fig. 2) and in Table 2 we present data for Young's modulus and the Bulk modulus. Notice that for the complete array of rocks presented in Table 2 the range is a factor of 10 from shales at one end of the spectrum to marble and dolomite at the other end. Thus a layer of sandstone or dolomite embedded in shale would not fold given the classical theory if driven solely by differences in elastic moduli.

Table 2
Young's modulus and bulk modulus for typical rock types (From Turcotte and Schubert, 1982)

Rock type	Young's modulus	Bulk modulus
	10^{11} Pa	10^{11} Pa
Shale	0.1–0.3	0.14
Sandstone	0.1–0.6	0.04–0.3
Limestone	0.6–0.8	0.2–0.3
Dolomite	0.5–0.9	0.3–0.5
Marble	0.3–0.9	0.2–0.35
Gneiss	0.4–0.7	0.1–0.35
Basalt	0.6–0.8	0.3
Granite	0.4–0.7	0.2–0.3
Anorthosite	0.8	0.35
Halite	0.7	0.3

3.2. Rate insensitive plasticity

If we assume that plasticity in rocks is represented by a Mohr–Coulomb constitutive relation (Vermeer and de Borst, 1984), then the two quantities that define the strength in compression are the cohesion, c, and the friction angle, φ. If the material behaves as a Drucker–Prager material then the relevant parameters that define the strength are related to the cohesion and friction; they are of the same order of magnitude for the two constitutive relations. Table 3 presents plasticity data for a range of rocks. The maximum principal stress, σ_1, at yield in compression is given by (see Ord, 1991)

$$\sigma_1 = p\frac{1+\sin\phi}{1-\sin\phi} + 2c\frac{\cos\phi}{1-\sin\phi} \tag{7}$$

where p is the confining pressure.

We arbitrarily consider a confining pressure of 100 MPa and the values for σ_1 are also given in Table 3. Again, the difference in strength for plastic materials is never more than 20 so that differences in competency arising from plasticity are not likely to produce folding. An exception could be massive basalt embedded in water saturated clay rich shales. The values reported in Table 3 are from Goodman (1980). Ord (1991) reports values for cohesion, friction angle and dilation angle based on experimental data from Edmond and Paterson (1972) and on an assumption that rocks behave as Mohr-Coulomb materials. Her tabulations for confining pressures up to 800 MPa (for marble) and 600 MPa (for sandstone) are compatible with the results reported by Goodman; her results also report data that follow the evolutionary behaviour of these parameters during deformation and with increased confining pressure. The friction angle decreases as confining pressure increases whereas the cohesion increases but still remain in the ranges reported in Table 3. For folding to develop in rocks with plastic constitutive behaviour, processes other than the Biot type of process need to operate such as the development of localised shear zones or fold packets.

3.3. Viscosity

We explore three geologically realistic possibilities here for power-law viscous materials. The constitutive law is given by

$$\dot{\varepsilon}_{ij} = A\sigma'^{N}_{ij}(3J_2)^{\frac{N-1}{2}}\exp\left[\frac{-Q}{RT}\right]\left(\frac{d}{d_o}\right)^{\delta} \tag{8}$$

where A is a material constant, Q is the activation enthalpy, R is the gas constant, d is the grain size in microns, d_o is a reference grain size and δ the grain size exponent; N is a material constant known

Table 3
Cohesion, friction angle and compressive strength at 100 MPa confining pressure for typical crustal rock types assuming Mohr–Coulomb behaviour (from Goodman, 1980)

Rock type	Cohesion	Friction angle	Confining pressure range	Compressive strength
	MPa	Degrees	MPa	MPa at 100 MPa confining pressure
Berea sandstone	27.2	27.8	0–200	92.9
Muddy shale	38.4	14.4	0–200	100.7
Edmonton bentonitic shale (with 30% water)	0.3	7.5	0.1–3.1	2.0
Sioux quartzite	70.6	48.0	0–203	367.9
Georgia marble	21.2	25.3	5.6–68.9	69.4
Chalk	0	31.5	10–90	3.2
Blaine anhydrite	43.4	29.4	0–203	151.5
Stone Mtn granite	55.1	51.0	0–68.9	319.2
Nevada test site basalt	66.2	31.0	3.4–34.5	237.1

as the *stress exponent*. J_2 (defined in equation (11)) is the second invariant of the deviatoric stress tensor, σ'_{ij} which is given by

$$\sigma'_{ij} \equiv \sigma_{ij} + p\delta_{ij} \tag{9}$$

where

$$p = -\tfrac{1}{3} trace(\sigma_{ij})$$

is the trace of the Cauchy stress tensor, σ_{ij}, or the pressure. Some values for A, Q and N are given in Tables 4 and 5. Notice that N is generally less than 5; an exception is coarse grained marble where $N = 7$–8.

The first possibility explored here involves quartzite embedded in marble, the second involves feldspathic material embedded in quartzite and the third involves wet diabase embedded in feldspathic material. The constitutive parameters are given in Table 4 and the resultant viscosity ratios are given graphically for feldspathic material embedded in quartzite in Fig. 4. For geologically realistic conditions, the viscosity ratio never exceeds 20. Calculations show that for the other rock assemblages, the viscosity ratios are not sufficient to drive folding or boudinage instabilities. An exception is quartzite embedded in marble (with $d_o = 1$ μm) with a stabilised grain size of 1 μm at temperatures of 600 K and strain-rates of 10^{-13} s^{-1} where the viscosity ratio is 905. Under these same conditions at a stabilised grain size of 10 μm the viscosity ratio is reduced to 69. In Fig. 4 the effective viscosity, η_{eff} is defined as

$$\eta_{eff} = \frac{\sqrt{3J_2}}{\dot{\varepsilon}} \tag{10}$$

where J_2 is the second invariant of the deviatoric stress and $\dot{\varepsilon}$ is the strain-rate. J_2 is given by (Jaeger, 1969)

$$J_2 = \frac{1}{6}\left[(\sigma_1 - \sigma_2)^2 + (\sigma_2 - \sigma_3)^2 + (\sigma_3 - \sigma_1)^2\right] \tag{11}$$

The effective viscosity defined in equation (10) is the secant effective viscosity (see Smith, 1977, Fig. 3). For power law viscous materials there is another measure of the effective viscosity, namely, the tangent effective viscosity, $\partial\sigma/\partial\dot{\varepsilon}$. This is equal to η_{eff}/N. Thus the ratio of effective tangent viscosities is N_e/N_L of the ratio of effective secant ratios and hence of much the same magnitude, but smaller, for constitutive parameters considered here.

It is clear from Fletcher (1974), Smith (1977) and equation (5) that the growth rates for folds involve the stress exponent, N, as an important parameter. Some experimental values of these are listed in Tables 4 and 5. Values of $N > 5$ are not common.

The important point, as the analysis of Mühlhaus et al. (1994) and Figs. 2 and 3 demonstrates, is that for any viscosity ratio the growth rates developed at small strains (where the linear theory holds) may not persist to high strains for constant strain rate or velocity boundary conditions. As the deformation proceeds the homogeneous component of the displacement field swamps the inhomogeneous field responsible for fold growth and the deformation field decays to homogeneous shortening with a consequent continued reduction in λ_D.

4. Thermodynamics of coupled thermal–mechanical behaviour

Most deforming systems in geology involve not only permanent distortion of the rock mass but are accompanied by fluid transport, chemical reactions and transport, and thermal transport. At least while the rock is actively deforming and mineral reactions are taking place, the system is not at equilibrium. A brief summary of the essential features of the theory of the deformation of materials with coupled processes involving fluid flow, chemical transport and reactions, and thermal transport is presented below within the framework of continuum non-equilibrium thermodynamics as developed by authors such as Callen (1960), Lavenda (1978), Ziegler (1983), Biot (1984), Coussy (1995, 2004), Maugin (1999) and Nguyen (2000). This is done to set the general scene and to indicate the way in which a varied array of processes operating in deforming rocks may be brought under one framework. We finally arrive at the Energy equation (19) which describes the temperature changes that arise from dissipative processes in a deforming rock mass. We then focus solely upon thermal processes for the purpose of this paper.

4.1. Postulate of local state

Our basic assumption is that the *postulate of local state* is relevant. This postulate says that in systems not at equilibrium, the state variables relevant for describing the state of the system at equilibrium are still relevant. It is not essential to do this but we adopt this approach for simplicity. Other approaches to non-equilibrium systems (so called Extended Non-Equilibrium Thermodynamics, Jou et al., 1993, and various gradient theories, Voyiadjis et al., 2003) have been developed where, in particular, *gradients* in these state variables are relevant to a description of the system not at equilibrium. For systems at equilibrium, gradients in state variables are usually not considered so that Extended Non-Equilibrium Thermodynamics and thermodynamic gradient theories represent a radical but realistic departure from the concepts of classical equilibrium thermodynamics. We adopt a more conservative approach.

4.2. Helmholtz Free Energy

The basis for tracking the energy fluxes in the coupled deforming system is the Helmholtz Free Energy density,

$$\Psi = e - Ts \tag{12}$$

Table 4
Constitutive parameters for models involving elastic-viscous–thermal coupling

Quantity	Description	Units	Quartzite[a]	Marble[b]	Feldspathic rock[c]	Wet diabase[c]
A	Pre exponential factor	Pa^{-N} s^{-1}	1.33×10^{-34}	5.01×10^{-6}	7.84×10^{-26}	7.94×10^{-20}
Q	Activation enthalpy	J mol^{-1}	135×10^3	190×10^3	163×10^3	276×10^3
N	Stress power law exponent	–	4	1.7	3.1	3.0
δ	Grain size exponent	–	0	−1.9	0	0
	Bulk modulus of layer in Fig. 3	Pa	4.66×10^{10}			
	Shear modulus of layer in Fig. 3	Pa	2.8×10^{10}			
	Bulk modulus of embedding medium in Fig. 3	Pa	2.33×10^9			
	Shear modulus of embedding medium in Fig. 3	Pa	1.4×10^9			

[a] Hirth et al. (2001).
[b] Walker et al. (1990).
[c] Strehlau and Meissner (1987).

Table 5
Ranges in value of the stress exponent, *N*, for a number of crustal rock types where a power law experimental creep law has been established

Rock type	Stress exponent, *N*
Dry quartzite[a]	1.9–2.9
Wet quartzite[b]	4.0
Dry granite[a]	2.9–3.4
Wet granite[a]	1.5
Dry diabase[a]	3.4
Wet diabase[a]	3.0
Coarse grained marble[c]	8.0
Marble[d]	5–7 high stress 3.3 medium stress 1.7 low stress

[a] Strehlau and Meissner (1987).
[b] Hirth et al. (2001).
[c] Heard and Raleigh (1972).
[d] Walker et al. (1990).

where e is the specific internal energy, s is the specific entropy and T is the absolute temperature. Ψ may also be written

$$\Psi = \Psi(\upsilon_k) \tag{13}$$

where υ_k is the array of k scalar, vector and tensor internal state variables that are capable of describing the system at equilibrium. If we incorporate more detail into equation (13) we can write Ψ as

$$\Psi = \Psi\left(\varepsilon_{ij}^{elastic}, \alpha_k, T\right) \tag{14}$$

where $\varepsilon_{ij}^{elastic}$ is the elastic strain tensor, and α_k is the collection of k scalar, vector and tensor internal state variables that describe the various physical and chemical processes accompanying the deformation. Notice that the total strain, ε^{total}, the plastic strain, $\varepsilon^{plastic}$, and the viscous strain, $\varepsilon^{viscous}$, are not thermodynamic state variables since all of these measures of strain are dependent upon the deformation history. In systems where these strains are independent of each other, that is, there are no feedback influences of elastic, plastic and viscous processes, these strains can be written in an additive manner (see Regenauer-Lieb et al., 2007):

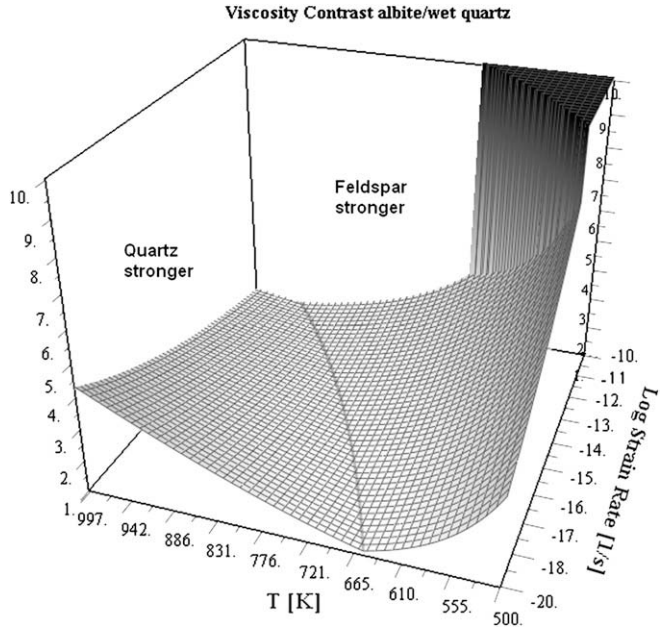

Fig. 4. Plot of contrasts in effective viscosity against temperature and strain-rate for feldspathic material embedded in quartzite. Constitutive parameters are given in Table 4.

$$\varepsilon^{total} = \varepsilon^{elastic} + \varepsilon^{plastic} + \varepsilon^{viscous} \tag{15}$$

In equation (15) we assume that the only deformation processes that dissipate energy (i.e. are converted to heat or sound and not stored in the material) are the plastic and viscous processes and we write:

$$\varepsilon^{dissipative} = \varepsilon^{plastic} + \varepsilon^{viscous} \tag{16}$$

However, for systems where there is coupling between these various mechanisms, as there is for instance when plastic damage is coupled to non-linear elasticity, one should consult Collins (2002), Maugin (1999) and Ben-Zion and Lyakhovsky (2006). For this paper we assume equations (15) and (16) are true.

One of the α_i may for instance be the mass, m_K, of the Kth chemical component in the system. Then, the chemical potential of this component, μ_K, is given by $\mu_K = \partial\Psi/\partial m_K$. In a similar fashion, if another α_i is ζ,the variation in fluid content in the porous system (see Detournay and Cheng, 1993), then the fluid pressure is given by $p_f = \partial\Psi/\partial\varsigma$. Other classical state variables, such as the Cauchy stress, σ_{ij}, and the specific entropy, s, are given by $\sigma_{ij} = \partial\Psi/\partial\varepsilon_{ij}^{elastic}$ and by $s = -(\partial\Psi/\partial T)$ respectively. Similar extensions can be made to include damage, grain size, crystallographic preferred orientation and dislocation concentration as various additional α_i (see Lyakhovsky and Ben-Zion, 1997; Shizawa and Zbib, 1999; Voyiadjis et al., 2003; Abu Al-Rub, 2004; Hamiel et al., 2004). Thus the Helmholtz Free Energy together with evolution equations, and constitutive relations to be discussed below, contain all of the information needed to describe the processes involved in the fully coupled deforming system with damage, thermal, fluid and chemical feedback processes operating.

4.3. Constitutive equations and evolution laws

Additional components of the description of the fully coupled system are the constitutive relations that describe the relations between stress and strain or strain-rate, and the relations that describe heat, fluid and chemical transport in the system. These latter relations are those of Fourier, Darcy and Fick, respectively. If the constitutive law that describes the deformation involves yield, damage or fabric development then there also needs to be a yield surface that defines the conditions under which the material is elastic or at yield, and a relation (the flow rule) that describes how the increment of inelastic strain-rate is related to the stress together with prescriptions of the evolution of and controls on damage and fabric. These constitutive and evolution laws, even if of an empirical nature, clearly must satisfy the Second Law of Thermodynamics which is expressed by the Clausius–Duhem Inequality. Indeed, in many instances the classical constitutive equations and evolutionary laws may be derived directly from the laws of thermodynamics and the Helmholtz Free Energy. Thus the yield function for plastic strain-rate insensitive materials is the Legendre Transform of the Dissipation Function (Collins and Houlsby, 1997; Houlsby and Puzrin, 2000) and the evolution of plastic strain follows directly from the orthogonality principle of Ziegler (Ziegler, 1983; Collins and Houlsby, 1997) that says that *the actual state of the thermodynamic forces operating in a non-equilibrium system is that which maximises the dissipation function over all other thermodynamically possible admissible states*. We describe the constitutive law used in this paper in Section 5.

4.4. First Law of Thermodynamics

Local conservation of energy within a non-reactive, dry system is expressed by the following form of the First Law of Thermodynamics (Truesdell and Toupin, 1960),

$$\rho\dot{e} = \sigma_{ij}\dot{\varepsilon}_{ij} - \frac{\partial q_i}{\partial x_j} + r \tag{17}$$

where ρ is the density, $\dot{e}$ is the time derivative of the specific internal energy which appears in the Helmholtz Free Energy, q_i is the heat flux vector, and r is the heat supply per unit mass generated by internal sources such as radioactive decay. We assume $r = 0$ in this paper. Expressions of the First Law for deforming continua with coupled fluid flow (both single and multi-phase), phase changes, chemical reactions, dissolution and precipitation and phase transitions are given by Coussy (1995, 2004).

4.5. The Second Law of Thermodynamics and the Clausius–Duhem Inequality

The Second Law of Thermodynamics for non-equilibrium processes is given by the Clausius–Duhem Inequality (Truesdell and Noll, 1965) which states that for the deformation of a specific reference volume the total dissipation must be positive:

$$\Phi^s \equiv T\frac{\partial s}{\partial t} = \left\{ \left[\sigma_{ij}\dot{\varepsilon}_{ij}^{dissipative} - \rho\left(\frac{\partial \Psi}{\partial t} + s\frac{\partial T}{\partial t}\right)\right] - \frac{q_i}{T}\nabla_i T \right\} \geq 0 \tag{18}$$

where Φ^s is the specific dissipation. The orthogonality principle of Ziegler (1983) follows directly from the Second Law and *vice versa* (Martyushev and Seleznev, 2006).

4.6. The Dissipation Function

The expression in curly brackets in the Clausius–Duhem Inequality, equation (18), consists of two parts: (i) that in square brackets represents the dissipation of energy due to deformation together with the other non-thermal processes operating in the system; and (ii) the dissipation of energy due to thermal conduction. The quantity in square brackets is known as the *Dissipation Function,* Φ. Since the quantity

$$\left\{ -\frac{q_i}{T}\nabla_i T \right\}$$

is always non-negative for a positive thermal conductivity, Φ is also always non-negative.

4.7. The Energy Equation

If we combine the expression for the First Law of Thermodynamics (equation (17)) with the definition of the Helmholtz Free Energy (equations (12) and (14)), and with the volumetric strain incorporated as a state variable, and use equations (15, 16) along with the expression $s = -(\partial\Psi/\partial T)$ then we arrive at the temperature equation. This equation describes the energy fluxes during deformation:

$$\rho c_p \frac{DT}{Dt} = \chi\sigma'_{ij}\dot{\varepsilon}_{ij}^{dissipation} - \alpha T\frac{Dp}{Dt} - \rho c_p \kappa\nabla^2 T \tag{19}$$

where c_p is the specific heat given by $c_p = T(\partial^2\Psi/\partial T^2)$ and $\alpha_{ij} = \rho(\partial^2\Psi/\partial\sigma_{ij}\partial T)$ (Nye, 1957). Although the thermal expansion is a tensor we assume spherical symmetry for the tensor here and represent it by the scalar α. The first term on the right of equation (19) describes shear heating arising from the mechanical dissipative processes. $\chi \leq 1$ is the Taylor–Quinney coefficient and represents the proportion of mechanical work arising from dissipative deformation that is available for heating or to drive diffusion, chemical reactions and structural adjustments. At high strains and low temperatures where the energy arising from deformation is stored in crystal defects, χ is generally in the range $0.85 \leq \chi \leq 1$ (Taylor and Quinney, 1934) and we take $\chi = 1$. The second term on the right of equation (19) describes the temperature change arising from isentropic work. The third term describes the temperature change arising from thermal conduction with thermal diffusivity, κ. Equation (19) is fundamental in describing the temperature changes that arise from the dissipative processes operating in a deforming rock mass.

5. Folding with coupled thermal–mechanical feedback

We employ an elastic-plastic von Mises yield function (Regenauer-Lieb and Yuen, 2003) together with a power law creep function such that the contributions to the total strain-rate, $\dot{\varepsilon}_{ij}^{Total}$, from the elastic, $\dot{\varepsilon}_{ij}^{elastic}$, plastic, $\dot{\varepsilon}_{ij}^{plastic}$ and creep, $\dot{\varepsilon}_{ij}^{creep}$, strain-rates, are additive:

$$\dot{\varepsilon}_{ij}^{Total} = \dot{\varepsilon}_{ij}^{elastic} + \dot{\varepsilon}_{ij}^{plastic} + \dot{\varepsilon}_{ij}^{creep} \tag{20}$$

or,

$$\dot{\varepsilon}_{ij}^{Total} = \left(\frac{1+\nu}{E}\frac{D\tilde{\sigma}'_{ij}}{Dt} + \frac{\nu}{E}\frac{Dp}{Dt} + \alpha\frac{DT}{Dt}\delta_{ij}\right)^{elastic} + \left(\dot{\varepsilon}_{ij}^{plastic}\frac{\sigma'_{ij}}{2\tau}\right)^{plastic} + \left(A\sigma'_{ij}(3J_2)^{\frac{N-1}{2}}\exp[-\frac{Q}{RT}]\right)^{creep} \tag{21}$$

where E is Young's modulus, ν is Poisson's ratio and α is the coefficient of thermal expansion. The operator D/Dt denotes the material derivative. $\tilde{\sigma}'_{ij}$ is the objective co-rotational stress and δ_{ij} is the Kronecker delta. A and N are power law material constants, Q is the activation enthalpy and R is the gas constant. J_2 is the second invariant of the deviatoric stress tensor, σ'_{ij}, defined by equation (9). τ is the yield stress.

The governing equations then are firstly the Continuity equation:

$$\frac{\partial\rho}{\partial t} + \rho\nabla \bullet \boldsymbol{u} = 0 \tag{22}$$

where $\boldsymbol{u}$ is the local material velocity vector. The continuity equation incorporates time as a derivative and so is coupled to the Energy equation (19). Secondly, the momentum equation describes equilibrium of forces:

$$\nabla \bullet \sigma_{ij} + \boldsymbol{f} = 0 \tag{23}$$

where $\nabla \bullet \sigma_{ij}$ is the divergence of the Cauchy stress tensor and $\boldsymbol{f}$ is the body force.

Two competing physical processes are essential for thermal–mechanical instabilities to develop; one involves the energy stored during deformation and the other, the energy dissipated during deformation. The rock matrix stores energy as it deforms by elastic deformation of the crystalline structure and by producing microstructural defects such as dislocation arrangements, micro-cracks or grain size changes. These processes are expressed as strain-hardening. The second process is the dissipation of energy, which appears as heat. This in turn weakens the material if temperature dependent processes dominate. For deformation modelled by equation (8) the effective viscosity, η_{eff}, within a one dimensional shear zone is described (Yuen et al., 1978; Fleitout and Froidevaux, 1980) by

$$\eta_{eff} \approx 8\kappa\rho c_p \frac{R\,T_c}{Q\,\dot{\varepsilon}^2 k^2} \tag{24}$$

where T_c is a critical temperature, and $\dot{\varepsilon}$ is the instantaneous strain-rate within the shear zone of initial, but collapsing, thickness, k.

Equation (24) describes the temperature at the centre of this shear zone at the beginning of localisation and implies that an order of magnitude increase in strain-rate within such a shear zone leads to a viscosity decrease of two orders of magnitude. As the shearing progresses and heat is conducted from the shear zone, two processes operate: (i) the viscosity within the shear zone decreases through thermal–mechanical feedback, and (ii) the thickness changes until the heat generated within the shear zone balances that lost to the surrounding material by conduction. At this stage the shear zone has achieved its minimum effective viscosity and maximum strain-rate, $\dot{\varepsilon}_{\max}$, related by

$$\eta_{eff} \approx 2\rho c_p \frac{R\,T_c}{Q\,\dot{\varepsilon}_{\max}} \tag{25}$$

and a steady state width, l_{therm}, given by equation (26) below. Equation (25) is exact for Newtonian viscous flow ($N = 1$) and a good approximation for power law viscous flow (Fleitout and Froidevaux, 1980). While the analytical approaches based on linear stability analyses (Ogawa, 1987; Hobbs and Ord, 1988) give insight into the instabilities associated with shear zone development, numerical models are required to investigate details of the growth of these instabilities and how they may nucleate folds. Whether new instabilities can develop during folding, and whether their development has an influence upon fold shape or upon fold evolution, can at present only be addressed numerically. Details of the theory behind the results presented are given in recent papers (Regenauer-Lieb and Yuen, 2003; Regenauer-Lieb et al., 2006).

In the more realistic case with thermal-elasticity, equation (19) shows that the contribution from the isentropic power can be significant. It effectively reduces the required temperature rise from shear heating to only a fraction of a degree thus opening the possibility of thermal–mechanical feedback to all geological materials and not just the materials with a high activation enthalpy like olivine. Most of the calculations presented here consider thermal-elasticity, thus incorporating isentropic power production which acts as a booster to thermal–mechanical instabilities.

6. Modelling of folding with thermal–mechanical feedback

The fundamental scaling length for the thermal–mechanical shear heating feedback is the thermal diffusion length scale of the shear zone given by the thermal diffusion equation (Carslaw and Jaeger, 1959),

$$l_{therm} = 2\sqrt{\frac{\kappa}{\dot{\varepsilon}_{\max}}} \tag{26}$$

where κ is of the order of $10^{-6}\,m^2\,s^{-1}$ and $\dot{\varepsilon}_{\max}$ is the maximum shear strain-rate in the shear zones at quasi-steady-state (say $10^{-12}\,s^{-1}$). l_{therm} is therefore of the order of 2 km. Another way of considering this is to note that at a strain rate of $10^{-12}\,s^{-1}$ the heat generated by deformation in a cube of rock of side 1 km diffuses out of the cube by the time the strain reaches 25% unless processes at a smaller scale (such as chemical reactions and damage formation) consume that heat. This means however that thermal–mechanical feedback operating alone produces only large scale folding. Folding at a finer scale depends on the operation of other processes such as thermal expansion, chemical reactions and volume changes associated with chemical reactions (Regenauer-Lieb et al., in press). In this paper only thermal expansion is considered in producing folds at a finer scale than that predicted by equation (26). The scale of these fine scale structures is governed by the scale of heterogeneity of the thermal expansion coefficient.

The coupled set of equations (19), (21), (22) and (21) has been implemented within a finite element thermo-mechanical code (ABAQUS/Standard, 2000). Details of the numerical problems and approach used are given in Regenauer-Lieb and Yuen (2004).

6.1. Single layers

Folding behaviour in thermal–mechanical coupled systems is illustrated in a generic model that incorporates a variety of length scales. This enables the generation of folds spanning length scales from metres to kilometres. We reproduce examples at the intermediate scale. The initial length of this model is 13.2 km and the height is 3 km. A feldspathic layer of initial thickness 400 m is embedded in a quartz rich matrix. We present results for a single-layer model at temperatures between 510 K and 570 K. We have presented results for 530 K elsewhere (Hobbs et al., 2007). The models are initially isothermal rather than incorporating a geothermal gradient. Our rationale for this derives from a consideration of the thermal Peclet Number, $Pe^{thermal}$, which is the ratio of heat transport due to advection by the deforming material to heat transport by conduction. This non-dimensional number is given by

$$Pe^{thermal} = \frac{L^2 \dot{\varepsilon}^{Total}}{\kappa}$$

where L is the height of the model. In the models considered, $Pe^{thermal}$ begins at 0.9 increasing during deformation to >8.0. Thus heat is moved by the deforming material faster than by conduction so that the local temperature in the model stays constant except for temperature changes induced by the deformation. Although initial geothermal gradients could be considered here, as a means to facilitate an understanding of the mechanisms involved we have opted to neglect them. Fine scale heterogeneity is introduced by incorporating random thermal perturbations associated with a thermal expansion strain of the order of 10^{-9}. These initial perturbations act as white noise for thermal–mechanical instabilities, which in turn cause thermal strain five orders of magnitude larger than that of the random perturbations. Perturbations may be interpreted as small-scale compositional-fabric heterogeneities such as would arise in a natural assemblage of quartz, feldspar and mica. Although this is a realistic thermal–mechanical effect, the perturbations also have a pure computational meaning in that they allow thermal–mechanical instabilities to arise around perturbations rather than nucleating from numerical round-off errors that are strictly mesh sensitive. In all models the initial topography of the quartz-feldspar interface is perturbed following an elastic eigenmode analysis (first 20 modes are perturbed) allowing the possibility for classical folding instabilities to develop, if this mechanism dominates.

We specifically explore the behaviour of a system in which there is initially a small difference in mechanical properties between the layer and the embedding matrix. The constitutive parameters are given in Table 4. At 540 K and a strain-rate of $10^{-13}\,s^{-1}$ the secant viscosity ratio is 3.2 (see Fig. 4) which in classical un-coupled theory would produce negligible fold amplification (see Fig. 3 of Sherwin and Chapple, 1968; Fig. 8 of Smith, 1977; Mühlhaus et al., 1994; and Fig. 2 of this paper). The tangent viscosity ratio is 2.5. The viscosity ratios for other conditions may also be read from Fig. 4.

Many constitutive relations for quartzites with different constitutive parameters to those selected here are tabulated by Evans and Kohlstedt (1995). Most of these give viscosity ratios at the conditions of interest larger than 3.2 quoted above (up to a ratio of 250); three give smaller ratios. The constitutive relation for quartzite is that selected by Hirth et al. (2001), after a critical analysis of the experimental data available, as most likely to represent natural behaviour. In accepting these constitutive

parameters from the available experimental data the point is made that this combination of parameters can never lead to folding by a Biot mechanism.

Fig. 5 shows results for single layer folding with no initial fine scale heterogeneity. The maximum ratio of the stress at this stage of deformation, is ~10. Large-scale ductile shear zones appear, arising from shear heating feedback, after 1 million years shortening. At this large scale shear heating feedback is the most efficient mechanism leading to instability. By this is meant that although the opportunity exists within the model setup for folds to develop by the classical un-coupled mechanism from initial geometrical perturbations driven by weak viscosity ratios, the perturbations induced by thermal–mechanical feedback grow fastest. At this scale, the intersections of developing shear zones with layer boundaries act as nucleation points for fold hinges. At these intersections the effective viscosity of the feldspar rich material is reduced due to shear heating in accordance with equation (25) and these weakened areas act as nucleation sites for localised buckles. In fact the viscosity in the feldspar layer in the inner side of the hinges is now smaller than the ambient viscosity in the embedding quartzite.

The reflection of shear zones off the bottom and top boundaries of the layer together with the inclination of shear zones at 45° to the bulk shortening axis means that the wavelength of folds that develop is of the order of $2h$, a factor of approximately 2 less than λ_D predicted by the analysis of Smith (1977, his Fig. 6) if such classical folds could grow.

Fig. 6 shows the results of shortening a single layer at temperatures between 510 K and 570 K and 10^{-15} s^{-1} imposed strain rate. The constitutive parameters are given in Table 4. No folds form at 510 K but fine scale crenulations are well developed. At the higher temperatures, folding develops along with axial plane crenulations. These crenulations are marked by distortion of the initial finite element grid and represent shear instabilities at a fine scale within an otherwise homogeneous matrix. They nucleate on the random distribution of thermal expansion perturbations initially distributed through the matrix. Because they arise within the matrix where all constitutive properties (other than the thermal expansion) are initially uniform, we refer to these crenulations as "passive structures". They correspond to the crenulations in colour bands of negligible strength difference commonly seen in quartzites or marbles. This transition from no folding at 510 K through

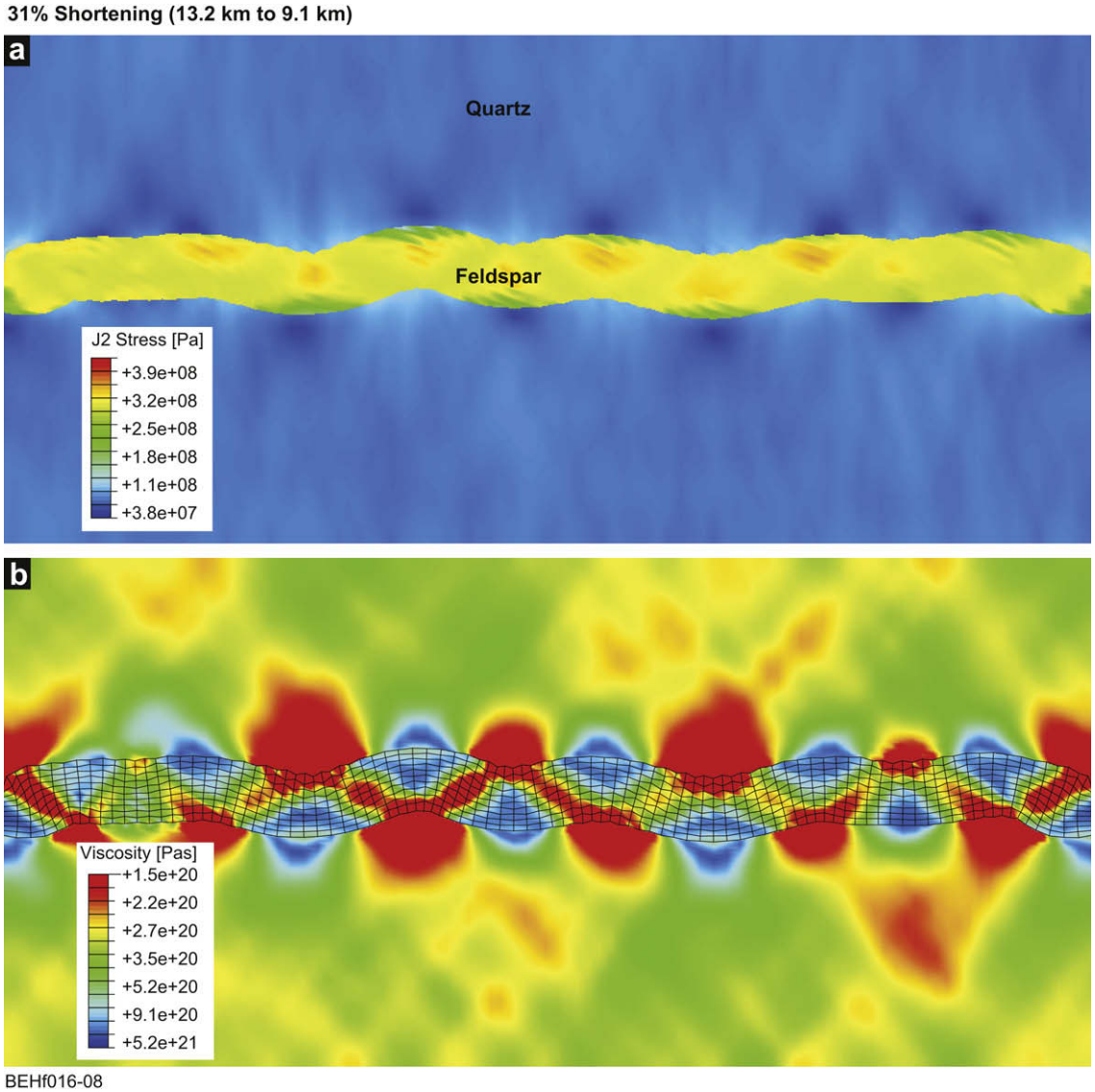

Fig. 5. Folding of feldspathic material embedded in quartzite at 530 K. 31% shortening of a layer initially 13.2 km long and 400 m thick. Shortening strain-rate is 10^{-14} s^{-1}. (a) Plot of stress. (b) Plot of effective viscosity.

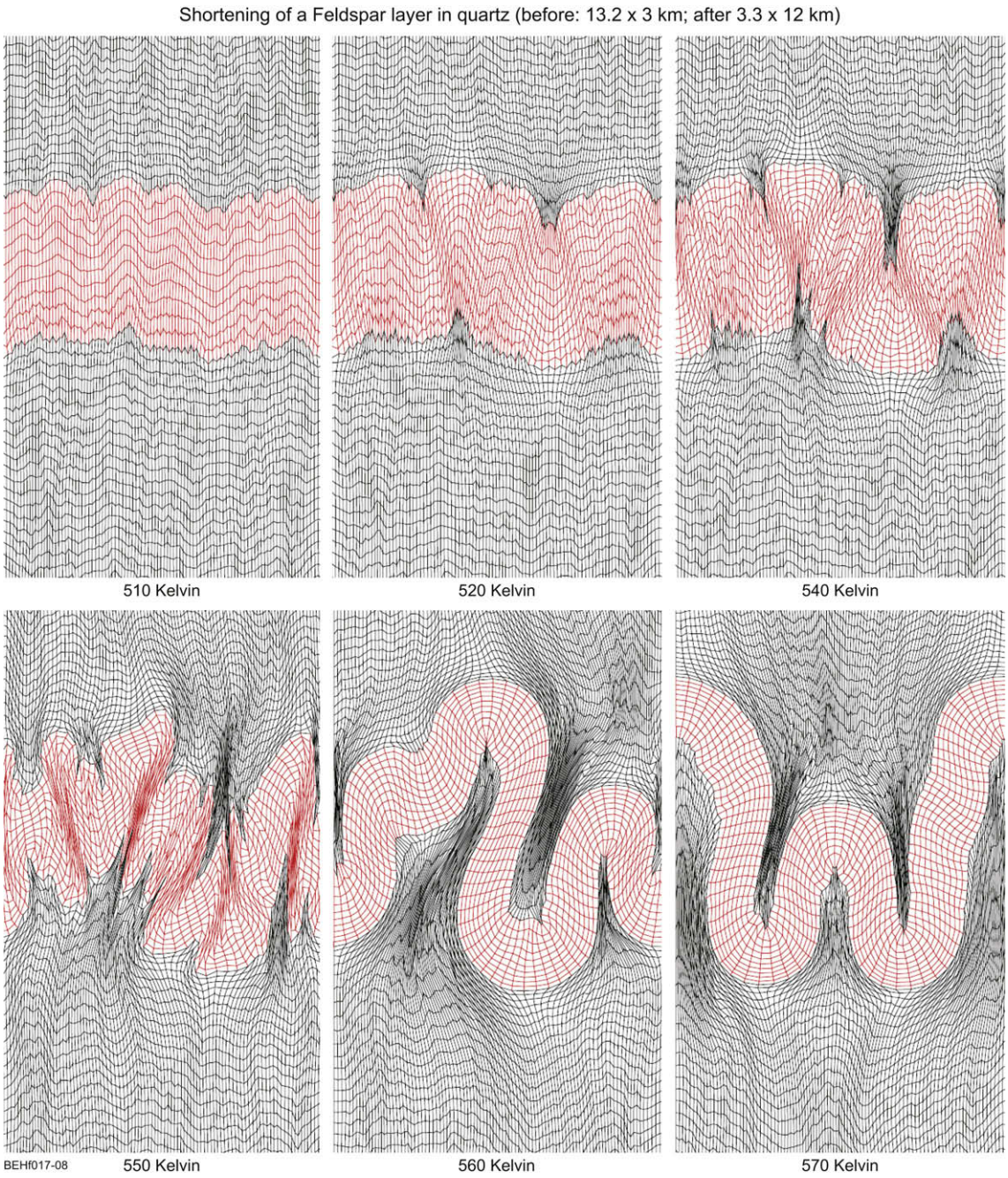

Fig. 6. Shortening of a single layer at temperatures between 510 K and 570 K. No folds develop until a critical temperature of approximately 530 K is reached.

somewhat brittle looking structures at 550 K to smooth, ductile folds at 560 K we believe represents a progression through the brittle-ductile transition.

Fig. 7 shows the geometry, viscosity and thermally induced strain after 76% shortening for the single layer case in which fine scale heterogeneity has been incorporated. Fig. 7a shows the viscosity and Fig. 7b shows zones of intense inhomogeneity of thermal strain developed parallel to the axial planes of the folds. These zones coincide with zones of viscosity difference as would be expected from equation (25). The thermal strain is defined as

$$\varepsilon_{ij}^{thermal} = \alpha \Delta T \delta_{ij} \tag{27}$$

where ΔT is the temperature rise within a shear zone. It is this distribution of thermal strain, and its influence on the local viscosity, that feeds back through equation (19) to produce the fine scale axial plane crenulations shown in Fig. 7b. Small-scale folding instabilities nucleate on the volumetric elastic expansion sites that have been inserted as thermal perturbations in the initial conditions. The folds become attenuated with strong shortening normal to the axial plane of the folds as shown in Fig. 8. The fold profiles are Type IA of Ramsay (1967). This contrasts with the nearly concentric profiles developed in un-coupled systems (for example: Zhang et al., 1996, 2000; Mancktelow, 2001; Schmalholz et al., 2001; Fig. 2 of this paper).

6.2. Multiple layers

Figs. 9 and 10 present the results of models in which two and ten layers are compressed. The constitutive parameters are given in

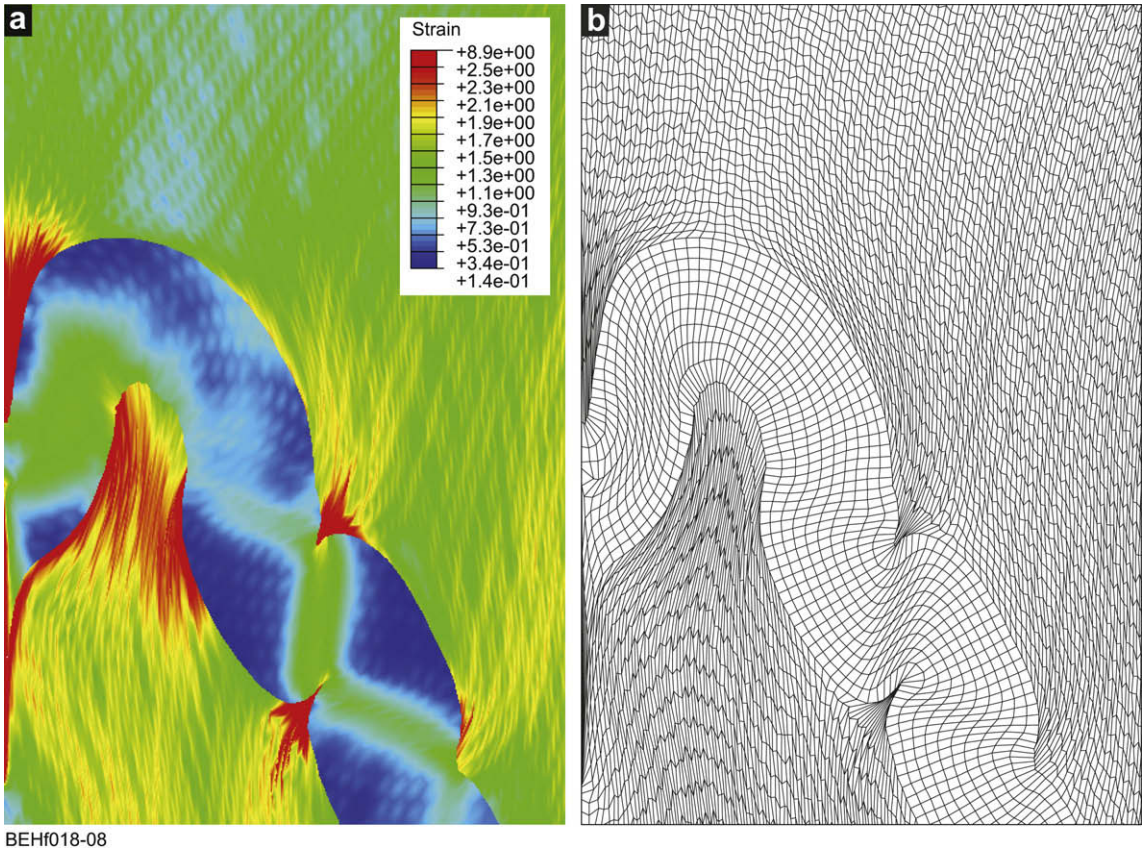

Fig. 7. Fine scale structure arising from thermally induced strains originating from initial heterogeneity in the thermal expansion coefficient. Temperature, 530 K; bulk strain, 76% shortening. (a) Distribution of strain. (b) Finer scale crenulations arising from initial heterogeneity of thermal expansion coefficient.

Table 4, the temperature is 530 K and the imposed strain-rate is 10^{-15} s^{-1}. The same basic features develop as for the single layer case. Shear bands nucleate within the competent layers at 45° to the layering. The effective viscosity is decreased within these shear bands and the intersection of shear bands with the layer boundaries then nucleates buckles at these weakened boundaries where the effective viscosity is up to 10 times *less* than in the rest of the layer. Notice again, as in the single layer case, the effective viscosity here is now less than that of the adjacent embedding medium. These shear bands are preserved to quite high strains (Figs. 9 and 10) and are responsible for the development of parasitic folds.

7. Discussion

This paper has been concerned with the deformation of layered rocks under conditions where thermal fluctuations, induced by deformation, have strong feedback influences upon the rheological properties. In general this will correspond to situations starting at mid-crustal levels and extending to deep in the crust and below into the mantle. We have shown that a large range of realistic structures arises through thermal–mechanical coupling. The important issue is that none of these structures would have arisen without such coupling since according to the analyses of Sherwin and Chapple (1968), Fletcher (1974), Smith (1975, 1977, 1979), Johnson and Fletcher (1994) and Mühlhaus et al. (1994) the viscosity ratios and/or the power law stress exponents of the material comprising the layers are too small to enable growth rates that would enable these structures to form at reasonable strains.

The folding process as such is quite distinct from the Biot buckling process. Thermal softening is concentrated into localised shear zones according to the mechanisms discussed by Fleitout and Froidevaux (1980). These shear zones produce more or less periodic intersections with the layering to induce localised zones of weakening that then act as nucleation sites for buckles. The important parameter involved is not the viscosity ratio but instead is the ratio in activation enthalpy of the layer to that of the embedding medium. The scale of folding produced by thermal–mechanical feedback is controlled by the ratio of the thermal diffusivity to the strain rate and hence for geological strain rates is in the range of hundreds to thousands of metres. However, fine scale heterogeneities that involve processes that liberate or absorb heat produce folding at a finer scale. These processes include volume changes associated with chemical reactions or thermal expansion as two examples. In this paper we have included fine scale heterogeneity in thermal expansion and this leads to fine scale folding in conjunction with coarse scale folding derived directly from thermal–mechanical feedback. The same fundamental processes operate with chemical-mechanical feedback where the scale of folding is controlled by the ratio of chemical diffusivity to the strain rate. For such chemical feedback processes folds develop at the scale of centimetres to millimetres (Regenauer-Lieb et al., in press).

It is natural to ask: *Are there other forms of coupling that could lead to similar structures perhaps in other parts of the crust?*

In the upper crust, in particular, fluid flow in porous rocks commonly accompanies deformation and, throughout the crust and mantle, chemical transport, and chemical reactions accompany deformation. The question is: do these processes also have an influence upon the development of structures during deformation of a similar character to those developed through thermal–mechanical coupling? The answer is a resounding *yes*. The detailed development of the influence of these feedback processes upon the

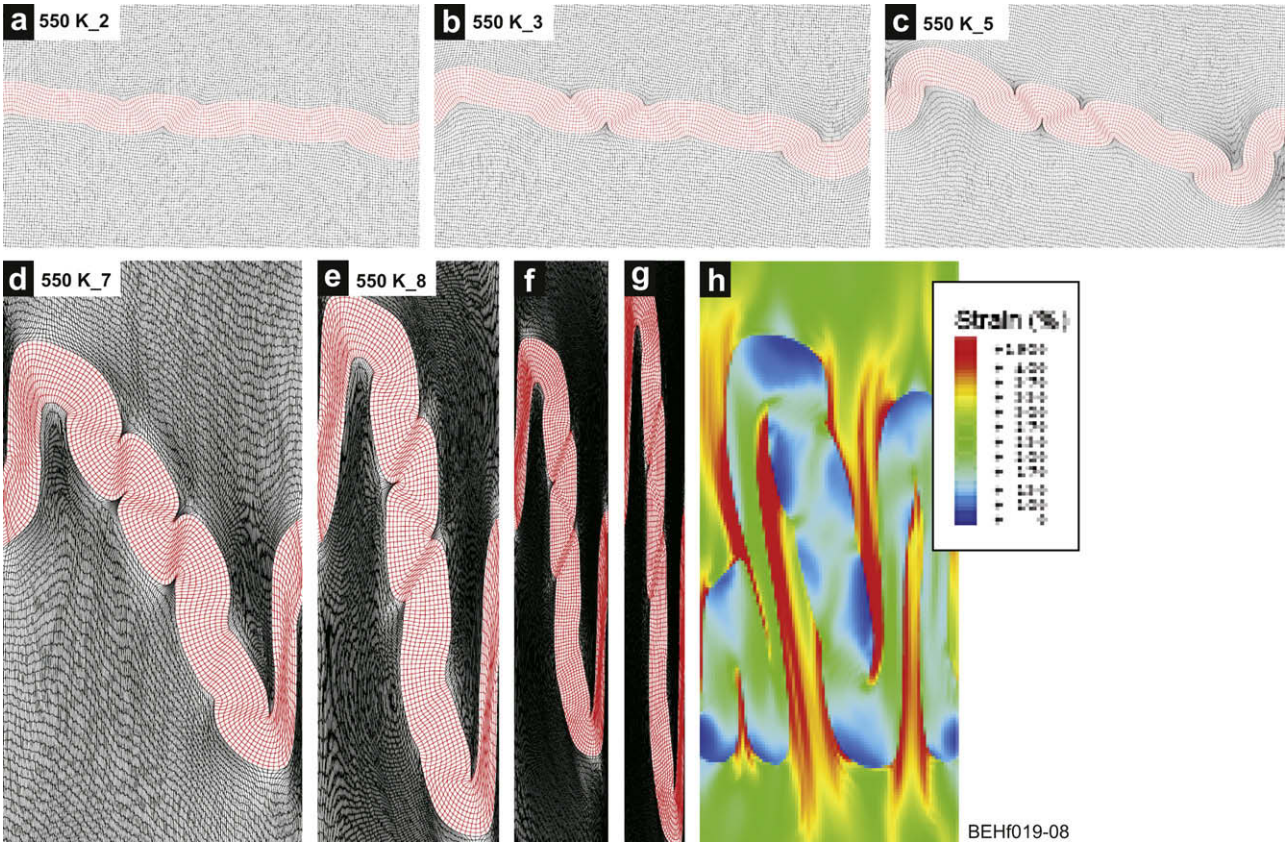

Fig. 8. Progressive shortening of a single layer at 550 K. Shortening is 26% in (a), 37% in (b), 47% in (c), 57% in (d), 67% in (e), 76% in (f), 76% in (g).

development of structures, fabrics and mineral assemblages in deforming rocks provides an overarching framework for understanding deformed and metamorphosed rocks and will be developed in subsequent papers. For the present, we give below a strongly abbreviated discussion of the deformation of systems in which fluid flow through a deforming, chemically reactive porous system is accompanying the deformation to give a flavour of the general framework governing deforming, chemically reactive systems with fluid flow.

The theoretical basis for considering processes operating in reactive, partially saturated deforming media is however in its infancy. A good summary of the state of the art, with references, is given by Coussy (1995, 2004).

For the case with no chemical reactions and single phase fluid flow and with K chemical components dissolved in the fluid, the non-thermal, mechanical part of the dissipation function, is

$$\Phi = \sigma_{ij}\dot{\varepsilon}_{ij} + \mu_K \frac{dm_K}{dt} \text{ (summation over the } K\text{s)} \tag{28}$$

whilst for the case with chemical reactions the non-thermal dissipation function is

$$\Phi = \sigma_{ij}\dot{\varepsilon}_{ij} + \mu_K \frac{dm_K}{dt} - J_K \bullet \left(grad\mu_K - \frac{\partial \mu_K}{\partial T} gradT \right) + \Phi_{chemical} \tag{29}$$

In equations (28) and (29), μ_K is the chemical potential of the Kth chemical component dissolved in the fluid, m_K is the mass of this component, J_K is the mass flux of the Kth chemical component and $\Phi_{chemical}$ is the dissipation due to the chemical reactions taking place during deformation. The symbol $\bullet$ represents the scalar product. Details are spelt out by Coussy (1995, 2004) but the important point is that these expressions have forms that are identical to that arising from thermal–mechanical coupling alone. If one considers non-isothermal situations, fluid flow and chemical reactions influence the heat produced during chemically reactive fluid flow and hence influence the fluid pressure and/or the viscosity of the deforming solid. Moreover, the chemical potential of chemical components in the reactive deforming system is influenced by stress, temperature and chemical concentrations so that gradients in chemical potential, and hence fluxes in chemical components, are an intrinsic part of the system.

Fluid–mechanical coupling depends upon the influence of pore pressure on the effective stress in the material, which in turn influences the deformation. There are two requirements here: (i) the material exhibits dilatancy and (ii) the constitutive relation is such that the effective stress has an influence on the deformation. Both of these features are true for common plastic constitutive laws such as Drucker–Prager and Mohr–Coulomb. If the material dilates with increasing deformation then the pore pressure decreases in the dilatant region leading to an increase in effective stress, a process known as *dilatancy hardening* (Rice, 1975).

Thus instability in fluid saturated materials depends ultimately upon fluctuations in the fluid pressure and hence, in dilatant plastic materials, upon fluctuations in the effective stress. Note that Biot published one paper (Biot, 1964) in which folding of a layer with coupling to fluid flow was studied and an analogy drawn with thermoelastic effects. That paper indicated that coupling deformation to fluid flow produces folds with dominant wavelengths described by relationships identical to those involved in viscous systems with functions involving the fluid pressure replacing the viscosity.

In these same materials with chemical reactions, there is a contribution from the dissipation arising from the chemical reactions in addition that can influence the temperature of the fluid and hence influence the fluid pressure.

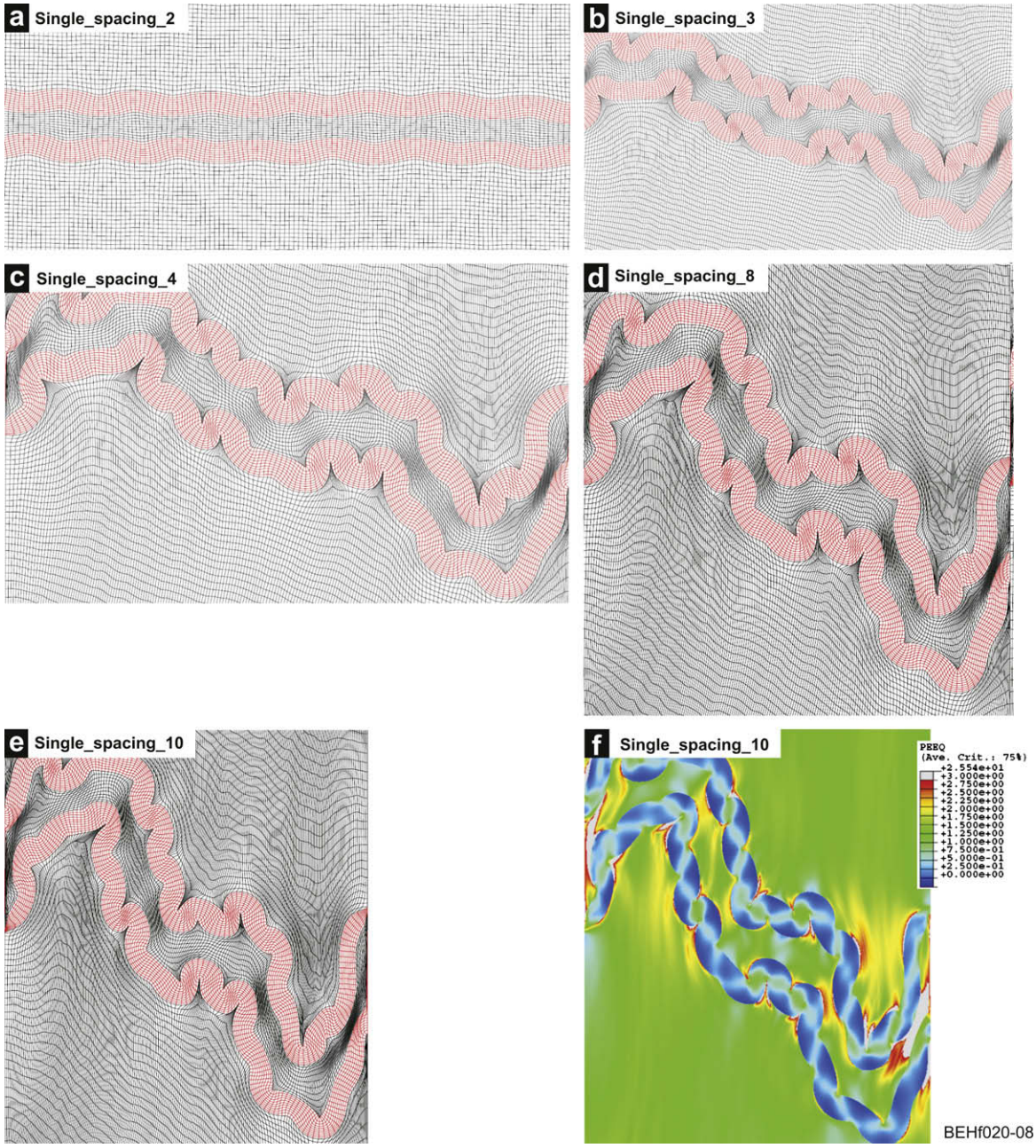

Fig. 9. Progressive shortening of two layers with initial spacing between the layers equal to layer thickness. Temperature 550 K. Shortening is 10% in (a), 40% in (b), 50% in (c), 55% in (d), 60% in (e), 60% in (f).

A quote from Biot (1974) summarises the situation and points to the unity that non-equilibrium thermodynamics brings to understanding the deformation of coupled systems (dots indicate words removed by the present authors);

> "The analysis of thermodynamic instability which is presented … in the context of thermal diffusion remains valid for the much more general case of unstable systems coupled with molecular diffusion of chemical species since they are governed by the same phenomenological Lagrangian equations of irreversible processes. For instance in the case of buckling, the bending deformation induces differences in chemical potentials of the molecular constituents between the regions in tension and compression, thus generating a diffusion and a creep buckling … This is also implicit in the physical meaning of viscoelasticity considered in the thermodynamic theory of initially stressed solids … Similarly … the theory of thermoelasticity is in complete analogy with the theory of porous solids, where a viscous fluid is allowed to diffuse through the pores. In this case the fluid pressure is the analogue of the temperature and the fluid flow corresponds to heat flow."

It is important to note that the systems examined by Biot are linear thermodynamic systems in the sense that thermodynamic fluxes such as heat flow or Darcy fluid flow are linear functions of thermodynamic forces, in these two cases, the gradients in temperature and hydraulic potential respectively; such relationships are common in processes relevant to geology. Moreover, the systems studied by Biot are stationary in that steady state

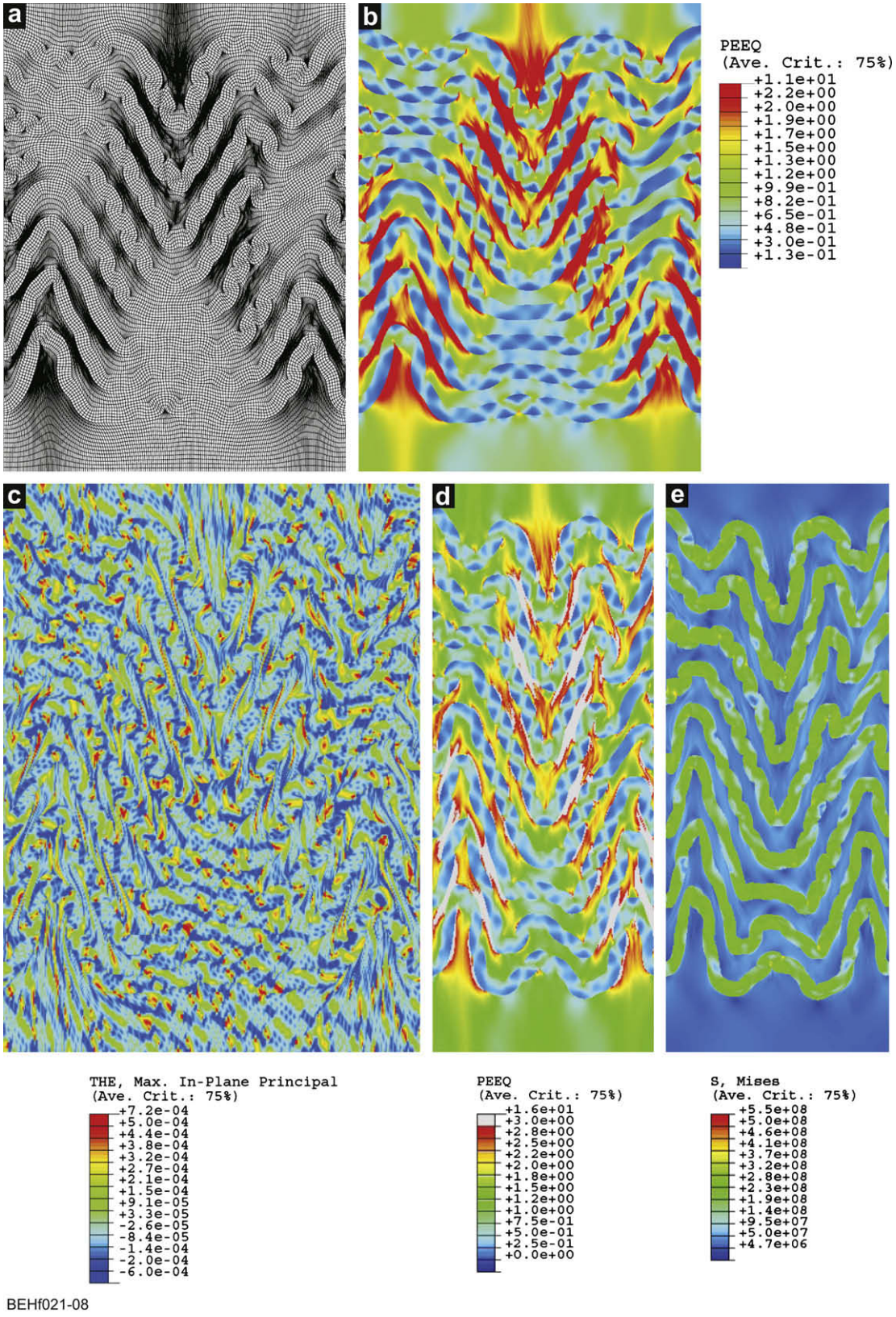

Fig. 10. Progressive shortening of a ten layer sequence with initial spacing between the layers equal to layer thickness. Temperature 550 K. Shortening is 40% in (a), grid is shown, 40% in (b), strain is shown, 45% in (c), thermal stain is shown, 55% in (d), strain is shown, 55% in (e), stress is shown.

conditions are assumed (Biot, 1955). Under such conditions, Prigogine's Principle of *Minimum Entropy Production* holds (Biot, 1955, 1958, 1974; Prigogine, 1955; Kondepudi and Prigogine, 1998). In the coupled systems described here, although linear in a thermodynamic sense, the systems are not stationary but evolve with time. Here the Principle of *Maximisation of Entropy Production* holds as proposed by Ziegler (1983). This is the more general situation for non-equilibrium systems; the Prigogine Principle is

a restricted sub-set of the Ziegler Principle (Martyushev and Seleznev, 2006). This represents the fundamental difference between the framework developed by Biot and that presented here.

8. Conclusions

8.1. Folding theory

The Biot theory of folding indicates that shortening of layered viscous materials results in the growth of a dominant wavelength, λ_D. The magnitude of λ_D depends on the layer thickness, h, the viscosity ratio between the layers and the embedding material, the amount of shortening and the boundary conditions. For constant force boundary conditions and Newtonian viscosity the amplification rates are exponential. λ_D is less than the Biot dominant wavelength, λ_B, for viscosity ratios less than 100 but for viscosity ratios greater than 100, $\lambda_D \approx \lambda_B$. In contrast, for viscosity ratios of approximately 20 and constant force boundary conditions λ_D/h is in the range for natural folds for 40% shortening and assumed amplification of about 100. However for constant velocity boundary conditions, the amplification rates are monotonically decreasing. $\lambda_D \approx \lambda_B$for viscosity ratios of 20 but the total amplification is small. $\lambda_D < \lambda_B$ for larger viscosity ratios and the established wavelength is progressively decreased by homogeneous shortening after amplification rates become small. λ_D/h ratios resembling those of natural folds are not developed at 40% shortening unless viscosity ratios are large ($\sim 10^3$). For both dynamic and kinematic boundary conditions significant amplification of folds does not develop for viscosity ratios less than approximately 10.

8.2. Natural viscosity ratios

Experimental data indicates that the viscosity ratios needed to drive the folding instability according to Biot type theories are too small in natural mid to lower crustal situations for folds to form. It may be that in some realistic situations such as quartzite embedded within weak shales, or pure coarse grained calcite embedded in stabilised very fine grained calcite, the viscosity ratios are high enough for the Biot theory to be applicable but in many instances especially in the mid to lower crust, other processes must operate.

8.3. Thermo-mechanical coupling

In this paper we have concentrated on thermal–mechanical coupling for rate (and temperature) sensitive elastic-plastic-viscous materials as one alternative to the Biot type of buckling mechanisms. Folds readily develop in these materials with realistic (that is, small, of the order of 2 times) ratios in effective viscosity. These instabilities are driven by feedback of heat generated by mechanical dissipation upon the viscosity of the material. Deformation leads to the development of shear zones within which the viscosity is reduced due to thermal softening. The intersection of these shear zones with layers produces localised areas of weakening that represent embryonic hinges that then buckle. The structures are realistic in that folds develop at a number of wavelengths, are of Type 1A or Type 3 at high strains and have axial plane structures well developed. One scale of folding developed by this process is controlled by the magnitude of the thermal diffusivity; the resultant wavelengths range from 100s to 1000s of metres. However, folds develop at finer scales arising from other dissipative processes such as thermal expansion. The scale of these structures is governed by the scale of heterogeneity of the coefficient of thermal expansion.

8.4. Other coupled processes

Although we have concentrated on thermal–mechanical coupling, it is clear from Biot's discussions that similar results are to be expected from fluid–mechanical and chemical-mechanical coupling. Although different physical–chemical processes are operating, the structure of the laws for thermal, fluid and chemical transport are identical (Fourier's, Darcy's and Fick's Laws, respectively). We propose that other processes may be equally important including damage, and microstructural and preferred orientation development. Combinations of these processes give insight into the development of structures at a range of length scales from the kilometre scale for thermal–mechanical feedback to the millimetre scale for chemical-mechanical feedback.

8.5. A unified theory

The general coupling between deformation and these other processes is fully unified within the concepts of non-equilibrium thermodynamics as developed by Biot (see Biot, 1984) and as extended and embellished by other workers (Ziegler, 1983; Coussy, 1995, 2004; Collins and Houlsby, 1997; Maugin, 1999; Nguyen, 2000; Abu Al-Rub, 2004) such that the Helmholtz Free Energy and the Dissipation Function are sufficient to describe the evolution of these systems. In subsequent papers we will explore these other damage–mechanical, fluid–mechanical and chemical–mechanical systems. The influence of chemical–mechanical feedback on the folding process has been discussed by Regenauer-Lieb et al. (in press) where folds on the scale of millimetres to centimetres are developed.

Acknowledgements

We thank Tom Blenkinsop, Ray Fletcher and Giles Hunt for comments that greatly improved this paper. The use of computational facilities at the Western Australian iVEC Computing Centre and the Minnesota Supercomputer Institute at the University of Minneapolis are gratefully acknowledged.

References

ABAQUS/Standard, 2000. User's Manual, Vol. 1. Hibbit, Karlsson and Sorenson Inc. Version 6.1.
Abbassi, M.R., Mancktelow, N.S., 1990. The effect of initial perturbation shape and symmetry on fold development. Journal of Structural Geology 12, 273–282.
Abbassi, M.R., Mancktelow, N.S., 1992. Single layer buckle folding in non-linear materials - I. Experimental study of fold development from an isolated initial perturbation. Journal of Structural Geology 14, 85–104.
Abu Al-Rub, R.K., 2004. Material length scales in gradient-dependent plasticity/damage and size effects: Theory and computation. PhD Thesis, Department of Civil and Environmental Engineering, Louisiana State University, 363 pp.
Anand, K.H.K., Kim, K.H., Shawki, T.G., 1987. Onset of shear localization in viscoplastic solids. Journal of the Mechanics and Physics of Solids 35, 407–429.
Ben-Zion, Y., Lyakhovsky, V., 2006. Analysis of aftershocks in a lithospheric model with seismogenic zone damage rheology. Geophysical Journal International 165, 197–210.
Biot, M.A., 1937. Bending of an infinite beam on an elastic foundation. ASME Journal of Applied Mechanics A59, 1–7.
Biot, M.A., 1955. Variational principles in irreversible thermodynamics with application to viscoelasticity. The Physical Review 97, 1463–1469.
Biot, M.A., 1957. Folding instability of a layered viscoelastic medium under compression. Proceedings of the Royal Society London A 242, 111–454.
Biot, M.A., 1958. Linear thermodynamics and the mechanics of solids. Proceedings Third U.S. National Congress of Applied Mechanics. Brown University, Providence, RI. ASME, New York, pp. 1-18.
Biot, M.A., 1959. On the instability of folding deformation of a layered viscoelastic medium in compression. Journal of Applied Mechanics 26, 393–400.
Biot, M.A., 1961. Theory of folding of stratified viscoelastic media and its implications in tectonics and orogenesis. Bulletin of the Geological Society of America 72, 1595–1620.
Biot, M.A., 1963. Internal buckling under initial stress in finite elasticity. Proceedings of the Royal Society London A 273, 306–328.
Biot, M.A., 1964. Theory of buckling of a porous slab and its thermoelastic analogy. Journal of Applied Mechanics Ser. E. E. 31, 194.
Biot, M.A., 1965. Mechanics of Incremental Deformations. John Wiley, New York, 504 pp.
Biot, M.A., 1974. Thermoelastic buckling. An unstable thermodynamic equilibrium at minimum entropy. Bulletin de l'Académie Royale de Belgique (Classe des Sciences), Ser. 5, Tome LX, 116–140.

Biot, M.A., 1984. New variational-Lagrangian irreversible thermodynamics with application to viscous flow, reaction-diffusion, and solid mechanics. Advances in Applied Mechanics 24, 1–91.
Carslaw, H.S., Jaeger, J.C., 1959. Conduction of Heat in Solids, second ed. Oxford University Press, London Oxford, 510 pp.
Callen, H.B., 1960. Thermodynamics: An Introduction to the Physical Theories of Equilibrium Thermostatics and Irreversible Thermodynamics. John Wiley and Sons, New York London, 376 pp.
Cobbold, P.R., 1975. Fold propagation in single embedded layers. Tectonophysics 27, 333–351.
Cobbold, P.R., 1976. Fold shapes as functions of progressive strain. Philosophical Transactions of the Royal Society London A 283, 120–138.
Collins, I.F., 2002. Associated and non-associated aspects of constitutive laws for coupled elastic/plastic materials. International Journal of Geomechanics 2, 259–267.
Collins, I.F., 2003. A systematic procedure for constructing critical state models in three dimensions. International Journal of Solids and Structures 40, 4379–4397.
Collins, I.F., Houlsby, G.T., 1997. Application of thermodynamical principles to the modelling of geotechnical materials. Proceedings of the Royal Society London A 453, 1975–2001.
Coussy, O., 1995. Mechanics of Porous Continua. Wiley, Chichester, UK, 472 pp.
Coussy, O., 2004. Poromechanics. Wiley, Chichester, UK, 298 pp.
Detournay, E., Cheng, A.H.-D., 1993. Fundamentals of poroelasticity. In: Hudson, J.A., Fairhurst, C. (Eds.), Comprehensive Rock Engineering, 2. Pergamon Press, Oxford, pp. 113–171.
Edmond, J.M., Paterson, M.S., 1972. Volume changes during the deformation of rocks at high pressures. International Journal of Rock Mechanics and Mining Science 9, 161–182.
Evans, B., Kohlstedt, D.L., 1995. Rheology of rocks. In: Ahrens, T.J. (Ed.), Rock Physics and Phase Relations. A Handbook of Physical Constants. American Geophysical Union, Washington, DC, pp. 148–165.
Fleitout, L., Froidevaux, C., 1980. Thermal and mechanical evolution of shear zones. Journal of Structural Geology 2, 159–164.
Fletcher, R.C., 1974. Wavelength selection in the folding of a single layer with power-law rheology. American Journal of Science 274, 1029–1043.
Fullagar, P.K., 1980. A description of nucleation of folds and boudins in terms of vorticity. Tectonophysics 65, 39–55.
Goodman, R.E., 1980. Introduction to Rock Mechanics. John Wiley, New York. 478 pp.
Hamiel, Y., Liu, Y., Lyakhovsky, V., Ben-Zion, Y., Lockner, D., 2004. A viscoelastic damage model with applications to stable and unstable fracturing. Geophysical Journal International 159, 1155–1165.
Heard, H.C., Raleigh, C.B., 1972. Steady state flow in marble at 500° to 800°C. Geological Society of America Bulletin 83, 935–956.
Hirth, G., Teyssier, C., Dunlap, W.J., 2001. An evaluation of quartzite flow laws based on comparisons between experimentally and naturally deformed rocks. International Journal of Earth Sciences 90, 77–87.
Hobbs, B.E., Ord, A., 1988. Plastic instabilities: implications for the origin of intermediate and deep focus earthquakes. Journal of Geophysical Research 93 (B9), 10521–10540.
Hobbs, B.E., Mühlhaus, H.-B., Ord, A., 1990. Instability, softening and localization of deformation. In: Knipe, R.J., Rutter, E.H. (Eds.), Deformation Mechanisms, Rheology and Tectonics. Geological Society Special Publication, No. 54, pp. 143–165.
Hobbs, B.E., Mühlhaus, H.-B., Ord, A., 2000. The influence of chemical migration upon fold evolution in multi-layered materials. In: Krug, H.-J., Kruhl, J.H. (Eds.), Non-Equilibrium Processes and Dissipative Structures in Geoscience. Selbstorganisation, 11, pp. 229–252.
Hobbs, B.E., Regenauer-Lieb, K., Ord, A., 2007. Thermodynamics of folding in the middle to lower crust. Geology 35, 175–178, doi:10.1130/G23188A.1.
Hobbs, B.E., Regenauer-Lieb, K., Ord, A., submitted for publication. The mechanics of boudinage formation. Journal of Structural Geology
Houlsby, G.T., Puzrin, A.M., 2000. A thermodynamic framework for constitutive models for rate-independent dissipative materials. International Journal of Plasticity 16, 1017–1047.
Hunt, G.W., Mühlhaus, H., Hobbs, B.E., Ord, A., 1996a. Localised folding of visco-elastic layers. Geologische Rundschau 85, 58–64.
Hunt, G.W., Mühlhaus, H.-B., Whiting, A.I.M., 1996b. Evolution of localized folding for a thin elastic layer in a softening visco-elastic medium. Pure and Applied Geophysics 146, 229–252.
Hunt, G.W., Peletier, M.A., Champnyes, A.R., Woods, P.D., Wadee, M., Budd, C.J., Lord, G.L., 2000. Cellular buckling in long structures. Nonlinear Dynamics 21, 3–29.
Hunt, G.W., Wadee, M.A., Ord, A., 2001. Length scale interactions in the folding of sandwich structures. Tectonophysics 335, 111–120.
Jaeger, J.C., 1969. Elasticity, Fracture and Flow. Methuen & Co. Ltd, London, 268 pp.
Jeng, F.S., Lai, Y.C., Teng, M.H., 2002. Influence of strain rate on buckle folding of an elasto-viscous single layer. Journal of Structural Geology 24, 501–516.
Jeng, F.S., Huang, K.P., 2008. Buckle folds of a single layer embedded in matrix-Theoretical solutions and characteristics. Journal of Structural Geology 30, 633–648.
Johnson, A.M., Fletcher, R.C., 1994. Folding of Viscous Layers. Columbia University Press, 461 pp.
Jou, D., Casas-Vazquez, G., Lebon, 1993. Extended Irreversible Thermodynamics. Springer, Berlin.
Kondepudi, D., Prigogine, I., 1998. Modern Thermodynamics. John Wiley, Chichester, 486 pp.
Lavenda, B.H., 1978. Thermodynamics of Irreversible Processes. MacMillan Press, 182 pp.
Lyakhovsky, V., Ben-Zion, Y., 1997. Distributed damage, faulting, and friction. Journal of Geophysical Research 102, 27635–277649.
Mancktelow, N.S., 1999. Finite-element modelling of single-layer folding in elasto-viscous materials: the effect of initial perturbation geometry. Journal of Structural Geology 21, 161–177.
Mancktelow, N.S., 2001. Single-layer folds developed from initial random perturbations: The effects of probability distribution, fractal dimension, phase and amplitude. In: Koyi, H.A., Mancktelow, N.S. (Eds.), Tectonic Modelling: A Volume in Honour of Hans Ramberg. Geological Society of America memoir 193, Boulder, CO, pp. 69–87.
Martyushev, L.M., Seleznev, V.D., 2006. Maximum entropy production principle in physics, chemistry and biology. Physics Reports 426, 1–45.
Maugin, G.A., 1999. The Thermomechanics of Non-linear Irreversible Behaviours. World Science.
Mühlhaus, H.-B., 1993. Evolution of elastic folds in plane strain. In: Kolymbas, D. (Ed.), Modern Approaches to Plasticity. Elsevier, New York, pp. 734–765.
Mühlhaus, H.-B., Hobbs, B.E., Ord, A., 1994. The role of axial constraints on the evolution of folds in single layers. In: Siriwardane, Zaman (Ed.), Computer Methods and Advances in Geomechanics. Balkema, Rotterdam, pp. 223–231.
Mühlhaus, H.-B., Sakaguchi, H., Hobbs, B.E., 1998. Evolution of three-dimensional folds for a non-Newtonian plate in a viscous medium. Proceedings of the Royal Society London A 454, 3121–3143.
Mühlhaus, H.-B., Moresi, L.N., Hobbs, B.E., Dufour, F., 2002. Large amplitude folding in finely layered viscoelastic rock structures. PAGEOPH 159, 2311–2333.
Neurath, C., Smith, R.B., 1982. The effect of material properties on growth rates of folding and boudinage: experiments with wax models. Journal of Structural Geology 4, 215–229.
Nguyen, Q.S., 2000. Stability and Nonlinear Solid Mechanics. Wiley, Chichester, UK, 398 pp.
Nye, J.F., 1957. Physical Properties of Crystals. Clarendon Press, Oxford, 322 pp.
Ogawa, M., 1987. Shear instability in a viscoelastic material as the cause of deep focus earthquakes. Journal of Geophysical Research 92 (B1), 13801–13810.
Ord, A., 1991. Deformation of rock: A pressure sensitive, dilatant material. PAGEOPH 137, 337–366.
Patton, R.L., Watkinson, J.A., 2005. A viscoelastic strain energy principle expressed in fold-thrust belts and other compressional regimes. Journal of Structural Geology 27, 1143–1154.
Price, N.J., Cosgrove, J.W., 1990. Analysis of Geological Structures. Cambridge University Press.
Prigogine, I., 1955. Introduction to the Thermodynamics of Irreversible Processes. Charles C. Thomas, Springfield, IL.
Ramberg, H., 1963. Fluid dynamics of viscous buckling applicable to the folding of layered rocks. American Association of Petroleum Geologists Bulletin 47, 484–505.
Ramsay, J.G., 1967. Folding and Fracturing of Rocks. McGraw-Hill, New York, 568 pp.
Regenauer-Lieb, K., Yuen, D.A., 2003. Modeling shear zones in geological and planetary sciences: solid- and fluid- thermal- mechanical approaches. Earth Science Reviews 63, 295–349.
Regenauer-Lieb, K., Yuen, D.A., 2004. Positive feedback of interacting ductile faults from coupling of equation of state, rheology and thermalmechanics. Physics of Earth and Planetary Interiors 142, 113–135.
Regenauer-Lieb, K., Weinberg, R.F., Rosenbaum, G., 2006. The effect of energy feedbacks on continental strength. Nature 442, 67–70, doi:10.1038/nature04868.
Regenauer-Lieb, K., Hobbs, B.E., Ord, A., Yuen, D.A., 2007. Non-equilibrium Thermodynamics, Thermomechanics, Geodynamics. Computational Science – ICCS 2007. 7th International Conference, Beijing, China, May 27–30, 2007. Lecture Notes in Computer Science, vol. 4487/2007, 62–69. DOI10.1007/978-3-540-72584-8_9.
Regenauer-Lieb, K., Hobbs, B.E., Ord, A., in press. Deformation with coupled chemical diffusion. Physics of the Earth and Planetary Interiors, doi:10.1016/j.pepi.2008.08.013.
Rice, J.R., 1975. On the stability of dilatant hardening for saturated rock masses. Journal of Geophysical Research 80, 1531–1536.
Schmalholz, S.M., Podladchikov, Y.Y., 1999. Buckling versus folding: Importance of viscoelasticity. Geophysical Research Letters 26, 2641–2644.
Schmalholz, S.M., Podladchikov, Y.Y., Schmid, D.W., 2001. A spectral/finite difference method for simulating large deformations of heterogeneous, viscoelastic materials. Geophysical Journal International 145, 199–208, doi:10.1046/j.o956-540x.2000.01371.x.
Sherwin, J., Chapple, W.M., 1968. Wavelength of single layer folds: A comparison between theory and observation. American Journal of Science 266, 167–179.
Shizawa, K., Zbib, H.M., 1999. A thermodynamical theory of gradient elastoplasticity with dislocation density tensor: I. Fundamentals. International Journal of Plasticity 15, 899–938.
Smith, R.B., 1975. A unified theory of the onset of folding, boudinage, and mullion structure. Bulleting of the Geological Society of America 86, 1601–1609.
Smith, R.B., 1977. Formation of folds, boudinage and mullions in non-Newtonian materials. Bulleting of the Geological Society of America 88, 312–320.
Smith, R.B., 1979. The folding of a strongly non-Newtonian layer. American Journal of Science 279, 272–287.
Strehlau, J., Meissner, R., 1987. Estimation of crustal viscosities and shear stresses from an extrapolation of experimental steady state flow data. In: Fuchs, K.,

Froidevaux, C. (Eds.), Composition, Structure and Dynamics of the Lithosphere-Asthenosphere System. AGU, GSA, pp. 69–87.
Taylor, G.I., Quinney, H., 1934. The latent energy remaining in a metal after cold working. Proceedings of the Royal Society A CXLIII, 307–326.
Truesdell, C., Toupin, R.A., 1960. The classical field theories. In: Flugge, S. (Ed.), Encyclopaedia of Physics, vol. 3/1. Springer-Verlag, Berlin, pp. 226–793.
Truesdell, C., Noll, W., 1965. The non-linear field theories of mechanics. In: Flugge, S. (Ed.), Encyclopaedia of Physics, vol. 3/3. Springer-Verlag, Berlin.
Turcotte, D.L., Schubert, G., 1982. Geodynamics. Wiley, New York, 450 pp.
Vermeer, P.A., de Borst, R., 1984. Non-associated plasticity for soils, concrete and rock. Heron 29, 1–64.
Voyiadjis, G.Z., Abu Al-Rub, R., Palazotto, A.N., 2003. Gradient dependent visco-plasticity and viscodamage. 16th ASCE Engineering Mechanics Conference, July 16–18, 2003, University of Washington, Seattle, pp. 1-12.
Walker, A.N., Rutter, E.H., Brodie, K.H., 1990. Experimental study of grain-size sensitive flow of synthetic, hot-pressed calcite rocks. In: Knipe, R.J., Rutter, E.H. (Eds.), Deformation Mechanisms, Rheology and Tectonics. Geological Society Special Publication No. 54, pp. 259–284.
Yuen, D.A., Fleitout, L., Schubert, G., Froidevaux, C., 1978. Shear deformation zones along major transform faults and subducting slabs. Geophysical Journal of the Royal Astronomical Society 54 (1), 93–119.
Zhang, Y., Hobbs, B.E., Ord, A., Mühlhaus, H.-B., 1996. Computer simulation of single layer buckling. Journal of Structural Geology 18, 643–655.
Zhang, Y., Mancktelow, N.S., Hobbs, B.E., Ord, A., Mühlhaus, H.-B., 2000. Numerical modelling of single-layer folding: clarification of an issue regarding the possible effect of computer codes and the influence of initial irregularities. Journal of Structural Geology 22, 1511–1522.
Ziegler, H., 1983. An Introduction to Thermomechanics, second ed. North-Holland Publishing Company, Amsterdam, 356 pp.